1 **Measurement report: Long-term measurements of aerosol precursor concentrations in the Finnish sub-**
2 **Arctic boreal forest**

3 Tuija Jokinen[1,2*], Katrianne Lehtipalo[1,3], Roseline Cutting Thakur[1], Ilona Ylivinkka[1], Kimmo Neitola[1], Nina
4 Sarnela[1], Totti Laitinen[1], Markku Kulmala[1], Tuukka Petäjä[1] and Mikko Sipilä[1]

5 [1]Institute for Atmospheric and Earth System Research (INAR) / Physics, Faculty of Science, University of
6 Helsinki, P.O. Box 64, Helsinki, 00014 University of Helsinki

7 [2]Climate & Atmosphere Research Centre (CARE-C), The Cyprus Institute, P.O. Box 27456, Nicosia, CY-
8 1645, Cyprus

9 [3]Finnish Meteorological Institute, Helsinki, Finland

10 *correspondence to t.jokinen@cyi.ac.cy

12 **Abstract:**

13 Aerosol particles form in the atmosphere by clustering of certain atmospheric vapors. After growing to larger
14 particles by condensation of low volatile gases, they can affect the Earth's climate by scattering light and by
15 acting as cloud condensation nuclei (CCN). Observations of low-volatility aerosol precursor gases have been
16 reported around the world but longer-term measurement series and any Arctic data sets showing seasonal
17 variation are close to non-existent. In here, we present ~7 months of aerosol precursor gas measurements
18 performed with the nitrate based chemical ionization mass spectrometer (CI-APi-TOF). We deployed our
19 measurements ~150 km North of the Arctic Circle at the continental Finnish sub-Arctic field station, SMEAR
20 I (Station for Measuring Ecosystem – Atmosphere Relations), located in Värriö strict nature reserve. We report
21 concentration measurements of the most common new particle formation (NPF) related compounds; sulfuric
22 acid (SA), methane sulfonic acid (MSA), iodic acid (IA) and a total concentration of highly oxygenated organic
23 molecules (HOMs). At this remote measurement site, SA is originated both from anthropogenic and biological
24 sources and has a clear diurnal cycle but no significant seasonal variation. MSA shows a more distinct seasonal
25 cycle with concentrations peaking in the summer. Of the measured compounds, IA concentrations are the most
26 stable throughout the measurement period, except in April, when the concentration of IA is significantly higher
27 than during the rest of the year. Otherwise, IA has almost identical daily maximum concentrations in spring,
28 summer and autumn, and on NPF event or non-event days. HOMs are abundant during the summer months
29 and low in the autumn months. Due to the low autumn concentrations and their high correlation with ambient
30 air temperature, we suggest that most of HOMs are products of biogenic emissions, most probably
31 monoterpene oxidation products. NPF events at SMEAR I happen under relatively low temperatures ($1 - 8$ ˚C)
32 with a fast temperature rise in the early morning hours, lower and decreasing relative humidity (RH, 55% vs.
33 80%) during the NPF days compared to non-event days. NPF days have clearly higher global irradiance values
34 (~450 m^{-2} vs. ~200 m^{-2}) and about 10 ppbv higher ozone concentrations than non-event days. During NPF
35 days, we have on average higher SA concentration peaking at noon, higher MSA concentrations in the
36 afternoon and slightly higher IA concentration than during non-event days. All together, these are the first long
37 term measurements of aerosol forming vapors from the SMEAR I in the sub-arctic region, and the results help
38 us to understand atmospheric chemical processes and aerosol formation in the rapidly changing Arctic.

39 **1. Introduction:**

40 The climate of sub-Arctic region is characterized with some of the most extreme temperature variations on
41 Earth. We expect that during the course of the 21st century, the boreal forest is to experience the largest increase
42 in temperatures of all forest biomes (IPCC, 2013), making it the most vulnerable to climate change. The boreal
43 forest (taiga) covers most of the sub-Arctic and encompasses more than 30% of all forests on Earth, being one
44 of the largest biome in the world (Brandt et al., 2013). The expected rate of changes, may overwhelm the
45 resilience of forest ecosystems and possibly lead to significant biome-level changes (Reyer et al., 2015). The

forest-atmosphere systems are closely interlinked to one another. The forest stores carbon and water in the peat, soil and as biomass while at the same time vegetation emits volatile organic compounds (VOC) into the atmosphere (Bradshaw and Warkentin, 2015). In the Arctic, summer is short, but solar radiation is abundant and extends the daylight hours all the way to midnight and beyond. On the other hand, during the polar night air pollutants accumulate in the atmosphere due to cold and stable atmosphere, while turbulent mixing is inhibited, and the lack of removal processes lead to the formation of Arctic haze (Stohl, 2006). These features make the Arctic an interesting study region for photochemistry of reduced atmospheric compounds. Oxidation processes that dominantly occur in the summer time control the processes removing VOCs and other traces gases, such as SO_2 and NO_x, from the atmosphere in the Arctic. Detailed understanding of atmospheric processes leading to aerosol precursor formation and gas-to-particle conversion and their role in feedback mechanisms help in assessing the future climate.

Aerosol and trace gas measurements in the sub-Arctic field station SMEAR I, go back to the 90s (Ahonen et al., 1997; Kulmala et al., 1998; Mäkelä et al., 1997). Trace gas and aerosol measurements at SMEAR I started in 1992 making them one of the longest continuous measurements of aerosol particle number and size distributions in the sub-Arctic (Ruuskanen et al., 2003). These long-term measurements show that aerosol particles regularly form and grow from very small sizes (< 8 nm diameter) with the highest frequency in the spring, between March and May (Dal Maso et al., 2007; Vehkamäki et al., 2004). It is suggested that spring promotes NPF because of the awakening of biological processes after the winter. At SMEAR I the snow only melts away in May-June and thus, many biological processes (photosynthesis) activate while the snow is still deep. This makes the Arctic spring a very complex environment for atmospheric chemistry with possible emission sources from melting snow, ice, melt water, vegetation and transport from other areas. At SMEAR I, most of the observed NPF events are either connected to clean air arriving from the Northern sector (originating from The Arctic Ocean and transported over boreal forest, Dal Maso et al., 2007) or the polluted air masses from the Eastern sector (Kyrö et al., 2014; Sipilä et al., 2021). Annually, around 30-60 NPF events are recorded at SMEAR I, of which around half could be initiated by anthropogenic air pollutants from the Kola Peninsula (Kyrö et al., 2014; Pirjola et al., 1998; Sipilä et al., 2021) leaving half of the events occurring from natural sources. The trend of NPF occurrence in Värriö is decreasing, as the anthropogenic sulfur dioxide emissions are decreasing in Russia (Kyrö et al., 2014).

Formation and growth of new particles at SMEAR I usually happen during daylight, highlighting the importance of photochemical activities. However, unlike most other locations, NPF is also observed during nighttime or polar night (Kyrö et al., 2014; Vehkamäki et al., 2004). Formation and growth processes of aerosols seem not to be correlated with each other at SMEAR I (Vehkamäki et al., 2004). Earlier literature reports that the formation rate (J) has no clear seasonal trend, while the growth rates (GR) of small particles clearly peak during summer (Ruuskanen et al., 2007). This indicates that different chemistry drives the initial cluster formation and the subsequent growth processes. From the observed nucleation rates it has been proposed that NPF at SMEAR I could be due to SA –ammonia (-water) nucleation (Napari et al., 2002) likely dominated by ion-induced channel at least during winter months (Sipilä et al., 2021). Kyrö et al., (2014) concludes that 20-50% of the condensational growth can also be explained by SA in Värriö. Other studies speculate about the possibility of different organic compounds participating in NPF in the sub-Arctic. Tunved et al., (2006) studied the air masses arriving to SMEAR I and concluded that the aerosol mass increased linearly with time that the air masses travelled over land. The concentration of condensing gases over the boreal forest was concluded to be high and most likely consisting mainly of oxidation products of terpenes (VOCs) that are emitted by the forest. At SMEAR II station in Hyytiälä, approximately 700 km South-West of Värriö, oxidized organics mostly explain the growth of newly formed particles (Bianchi et al., 2017; Ehn et al., 2014). However, direct measurements of the aerosol forming and growing vapor species are still lacking from SMEAR I except during wintertime without biogenic activity when SA has been shown to be primarily responsible on formation and growth (Sipilä et al., 2021). In Värriö, the role of NPF is critical in forming of CCN, since measurements show that the number of CCN can increase up to 800 % as a result of NPF (Kerminen et al., 2012). In other locations in the boreal forest and Arctic, some measurements shed light into the possible chemical components that could be forming particles in Värriö. Currently, the closest continuous measurements with the nitrate based

CI-APi-TOF are conducted in Hyytiälä at the SMEAR II-station (Jokinen et al., 2012, 2017; Kulmala et al., 2013). In Hyytiälä there is direct evidence on the key role of the photochemical production of SA and HOMs maintaining atmospheric NPF (Bianchi et al., 2017; Ehn et al., 2014; Jokinen et al., 2017; Kulmala et al., 2013).

Other chemical composition measurements of aerosol precursors have been conducted only in a few locations in the High-Arctic and over the Arctic Ocean (Baccarini et al., 2020; Beck et al., 2021; He et al., 2021; Sipilä et al., 2016). These studies show that in the Arctic, the marginal ice zone and the coast of the Arctic Ocean is a source of atmospheric IA that is efficiently forming new particles. SA and MSA concentrations were also reported (Beck et al., 2021), but they were much lower in concentration than IA (Baccarini et al., 2020). However, the chemistry behind NPF is not that simple, even in the pristine Arctic air. The clean air above the Arctic Ocean is abundant in dimethyl sulfide (DMS) emitted by phytoplankton that rapidly oxidizes into SA and MSA on sunny days and consequently forms CCN (Charlson et al., 1987; Park et al., 2018). Beck et al., (2021) report that in Svalbard in the Arctic Ocean, SA and MSA contribute to the formation of secondary aerosol. They also observed that these compounds formed particles large enough to contribute to some extent to CCN. This is supported by measurements of aerosol chemical composition from the Arctic that commonly report MSA in particulate matter (Dall Osto et al., 2018; Kerminen et al., 1997). According to Beck et al. (2021) the initial aerosol formation in the high Arctic occurs via ion-induced nucleation of SA and ammonia and subsequent growth by mainly SA and MSA condensation during springtime and HOM during summertime. By contrast, in an ice-covered region around Villum, Greenland, Beck et al. (2021) observed NPF driven by IA, but the particles remained small and did not grow to CCN sizes due to insufficient concentration of condensing vapors. Since the Arctic CCN number concentrations are low in general, formation of new particles is a very sensitive process affecting the composition of the aerosol population and CCN numbers in the area.

In this article, we present the measurements of aerosol precursor molecules from the continental SMEAR I station, ~150 km North of the Arctic Circle and ~150 km from the Arctic Ocean. We measured SA, MSA, IA and HOM concentrations with a SA calibrated CI-APi-TOF (Jokinen et al., 2012; Kürten et al., 2012) to determine their levels in the sub-Arctic boreal forest and to understand whether these species are connected with the aerosol formation process in the area.

2. Methods, measurement site and instrumentation:

The core of this work is measurements of gas phase aerosol precursors. We use the nitrate chemical ionization atmospheric pressure interface time-of-flight mass spectrometer (CI-APi-ToF) that has been operational at the SMEAR I-station (N67°46, E29°36) in Eastern-Lapland since the early spring of 2019. Measurements were done on top of Kotovaara hill (390 m a.s.l.), close to ground level in an air-conditioned small log wood cottage. The cottage is surrounded by ~65-year-old Scotts pine forest. More details about the station can be found in earlier publications (Hari et al., 1994; Kyrö et al., 2014). The mass spectrometric measurements are designed to start a long-term measurement series of atmospheric aerosol forming trace gases in the Finnish Lapland and the measurements are ongoing to this day. We measure e.g. SA, IA, HOMs and MSA with high time resolution and precision. The measurements are running in Finnish winter time (UTC+2) throughout the year.

We calibrated the CI-APi-TOF twice during the measurement period and run the instrument with the same settings for the whole measurement period reported in this paper. We calibrated the instrument using a SA calibrator described in Kürten et al. (2012). The calibration factor from the two separate calibrations were 1) $7 \cdot 10^9$ and 2) $8 \cdot 10^9$ and we use the average $7.5 \cdot 10^9$ in our study calculate the concentrations of all reported compounds. This factor includes the loss parameter due to the ~1 m long unheated inlet tube (3/4" stainless steel). HOMs and IA have been estimated to be charged similarly at the kinetic limit as SA (Ehn et al., 2014; Sipilä et al., 2016), so the calibration factor for them should be similar, but please note that the concentration of other compounds than SA can be highly uncertain due to different ionizing efficiencies, sensitivities and other unknown uncertainties. If MSA, IA or HOMs do not ionize at the kinetic limit these concentrations could be underestimated and thus, the concentrations reported in here should be taken as low limit values. The SA,

IA and MSA data presented in this study are all results of high-resolution peak fitting of the CI-APi-TOF, in order to avoid inaccurate identification of compounds and to separate overlapping peaks. The HOM data is a sum of mass-to-charge ratios from 300 to 400 Th, representing the monomer HOM range (C_{10} compound range), 401 to 500 Th for the slightly larger HOMs (C_{15} compound range) and 501 to 600 Th for the dimer species (C_{20} compound range). We also give the sum of these all (from 300 to 600 Th). The goal of this article is not to specify different HOM compounds or to study NPF in mechanistic details but to give an overview of general seasonal trends and variations of these selected species. Note that since this is a sum of all peaks in the selected mass range, we cannot assure that all the compounds included are HOMs. However, the investigation in laboratory conditions show that the nitrate-CI-APi-TOF is highly selective and sensitive towards HOMs with $O > 5$ (Riva et al., 2019) and with hydroperoxide (-OOH) functionalities (Hyttinen et al., 2015). All data obtained from the CI-APi-TOF we analyzed using tofTools program described in (Junninen et al., 2010) and averaged over an hour. The original data time resolution is 5 sec. The uncertainty range of the measured concentrations reported in this study is estimated to be $-50\%/+100\%$ and the limit of detection, LOD, $4 \cdot 10^4$ molecules cm^{-3} (Jokinen et al., 2012).

To classify NPF events recorded during the measurement period, we used the data measured by a Differential Mobility Particle Sizer (DMPS). Condensation sink was also calculated using the DMPS data. The DMPS instrument and earlier statistics of NPF events in Värriö has been documented by (Dal Maso et al., 2007; Vana et al., 2016; Vehkamäki et al., 2004). The NPF events were classified according to Maso et al., (2005). Total aerosol particle number concentration was measured with a Condensation Particle Counter (CPC, TSI 3776) in the size range of 3 – 800 nm. Air ion size distributions were measured with the Neutral cluster and Air Ion Spectrometer, NAIS (Kulmala et al., 2007; Manninen et al., 2016; Mirme and Mirme, 2013) that measures negative and positive ions in the size range of 0.8 – 42 nm in mobility diameter and total particle size distribution between ~2 and 42 nm.

3. **Results and discussion:**
   ### 3.1. Overview of the whole measurement period:

You can see a time series of the most common aerosol precursor compounds; SA, MSA, IA and sums of different HOM groups in Figure 1. This figure depicts the whole measurement period from April 4 to October 27 in 2019. Overall, we succeeded to measure the whole 7 month period almost uninterruptedly. Only a few short power cuts stopped our measurements during this time. IA data is missing from late July since its peak could not be separated well enough from overlapping peaks in the spectra during this time. This was due to poor resolution (low signal of IO_3^- close to another peak) that makes peak integration to give negative, unreal values and we thus decided to flag them out. After late October, the instrument malfunctioned and stopped our measurements. In this particular article, we present data from spring (Apr-May), summer (Jun-Jul-Aug) and autumn (Sep-Oct) 2019. More about the SMEAR I winter observations can be read in Sipilä et al., 2021 were they report observations of polar night pollution events from Värriö after the CI-APi-TOF was fixed.

179
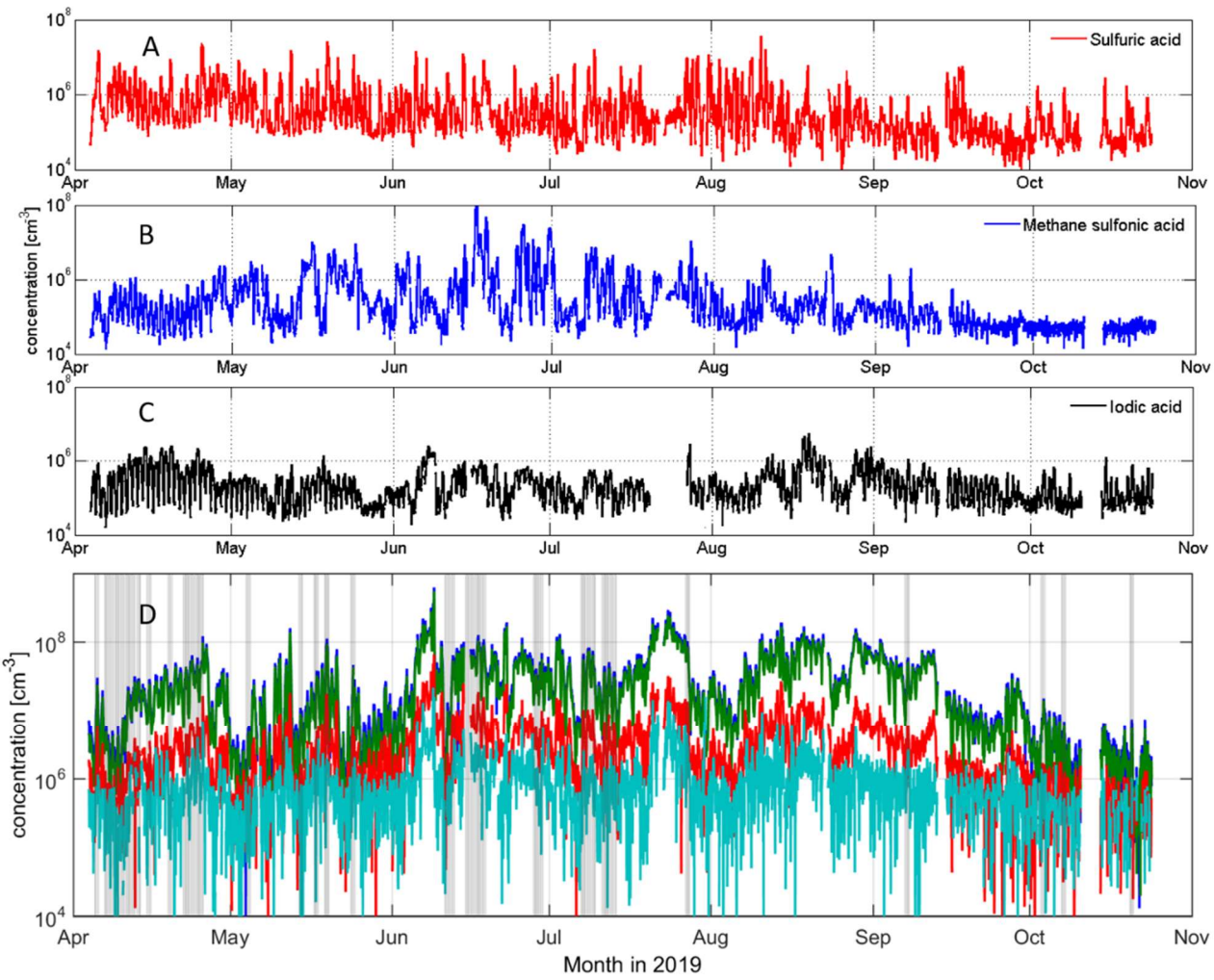
Figure 1. Overview of sulfuric (A), methane sulfonic (B) and iodic acid (C), as well as HOM (D) concentrations at SMEAR I in April to October 2019. NPF days are depicted in grey shading in panel D. All data in panels A-C are resulting from high-resolution peak fitting. HOM data are sums of certain mass ranges; from 300 to 400 Th in green, representing C10 or HOM monomer compounds, from 401 to 500 Th in red, representing C15 compound and from 501 to 600 Th on light blue, representing C20 or HOM dimer compounds. The sum of HOM (darker blue) is a sum of the aforementioned mass ranges. The sum of HOMs is approximately one order of magnitude higher than SA, MSA or IA concentrations during this measurement period.

In Figure 2 we show some of the most interesting environmental and meteorological parameters that influence the atmospheric gas composition during the measurements period; temperature, global radiation and snow depth, ozone, NO_x and SO_2 mixing ratios. There are some special features in year 2019; the summer had two heat waves, when the air temperature rose up to 29.2 °C in early June and to almost the same values in late July. These episodes are getting more common in Lapland due to climate change. These warmer conditions will probably change the emissions of trace gases including the composition and abundance of aerosol precursors in the future Arctic environment (Schmale et al., 2021). However, heath wave conditions are likely not favorable conditions to NPF since condensation of low-volatility gases is favored in colder temperatures (via the vapor pressure decrease due to lower temperatures), but they may affect the oxidation chemistry of VOCs by promoting dimer formation.

From Figure 2, we also see that the snow covered period ended in 2019 in late May and snow started to accumulate again in mid-October. Solar radiation (Figure 2A) is intense in Värriö during springtime and gives

Värriö favorable photo-oxidizing conditions, effectively removing air pollutants and trace gases from the atmosphere. Photochemical activity in presence of NO_x (Figure 2E), produces ozone in springtime and this is visible in very high ozone mixing ratios at the site (Figure 2D). Median ozone mixing ratios were around 55 ppbv in April and decreased to ~30 ppbv in the late summer and autumn. The spring ozone mixing ratio in 2019 was significantly higher than the previous reports from the years 1992 to 2001, when monthly mean values of ozone varied between 25 – 40 ppbv (Ruuskanen et al., 2003).

The springtime diurnal solar cycle is clearly visible with all studied compounds. All measured aerosol precursor compounds are abundant even during the period when snow covers the ground in the spring. The HOM concentrations follow the increasing solar radiation and rising temperature. MSA has a stronger diurnal cycle before the snow melt than after it. This may be due to rain and cloudy conditions that are more common in the summer. SA and IA do not have such strong seasonal variation than HOMs and MSA. The aerosol precursor concentrations are discussed in more detail in the following sections.

3.2. Seasonal and monthly variation of SA, MSA, IA and HOM concentrations

We present the diurnal variation of aerosol precursors; SA, MSA, IA and highly oxygenated molecules, concentrations separately for different seasons accompanied with solar radiation and total aerosol number concentrations in Figure 3. Strong seasonality is most evident in SA and HOM concentrations. SA is at its highest in the spring, decreasing toward summer and autumn while HOMs reach their maximum in the summer. We detect an increase in total aerosol number concentration on the spring evenings that is likely due to more frequent NPF events taking place at SMEAR I. The increase in HOMs in the summer at SMEAR I is linked to the increased emissions of VOCs from vegetation that oxidize into HOMs via ozonolysis (Ehn et al., 2014) and OH-radical reactions (Berndt et al., 2016; Jokinen et al., 2014, 2017; Wang et al., 2018). The overall lowest aerosol precursor concentrations and aerosol number concentration we detect during autumn (winter data was missing from this study, see Sipilä et al. 2021, for winter time observations made promptly after the period reported here). MSA shows very similar concentrations during spring and summer, and drops down to the limit of detection level for autumn. IA acts very differently than the other compounds. We observe IA to have a similar level of concentration throughout the measurement period and seems that the concentration reaches a steady state during daylight hours. This daytime maximum stays at the same level about 5 hours longer during spring than in the autumn. The day length getting shorter towards the autumn explains this behavior. The maximum hourly median concentrations for the measured compounds are ~$2 \cdot 10^6$ cm^{-3} for SA (spring), ~$5 \cdot 10^5$ cm^{-3} for MSA (summer), ~$3 \cdot 10^5$ cm^{-3} for IA (all seasons) and ~$5 \cdot 10^7$ cm^{-3} for the sum of HOMs (summer, mass range from 300 to 600 Th).
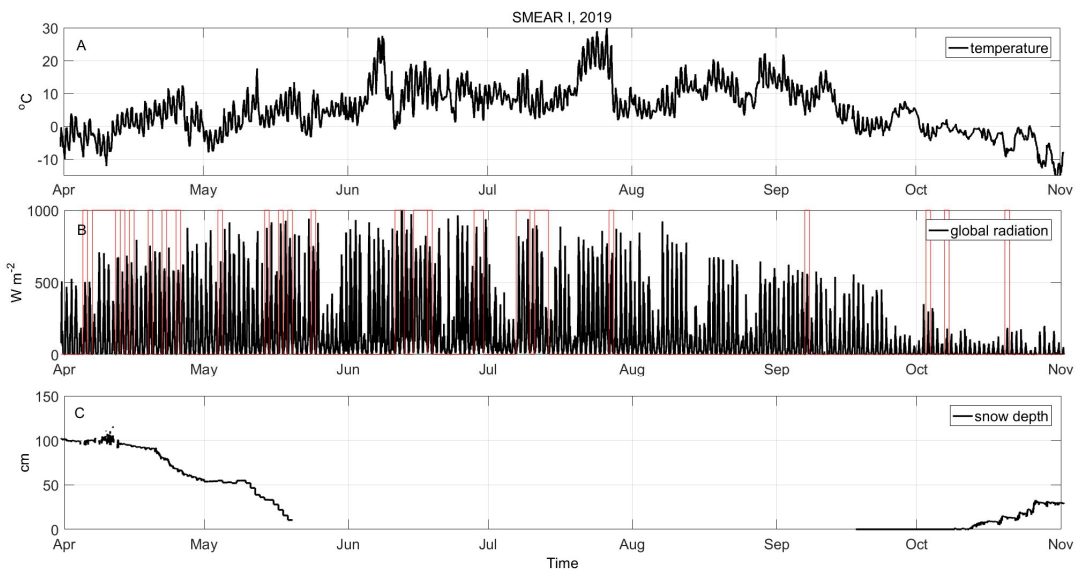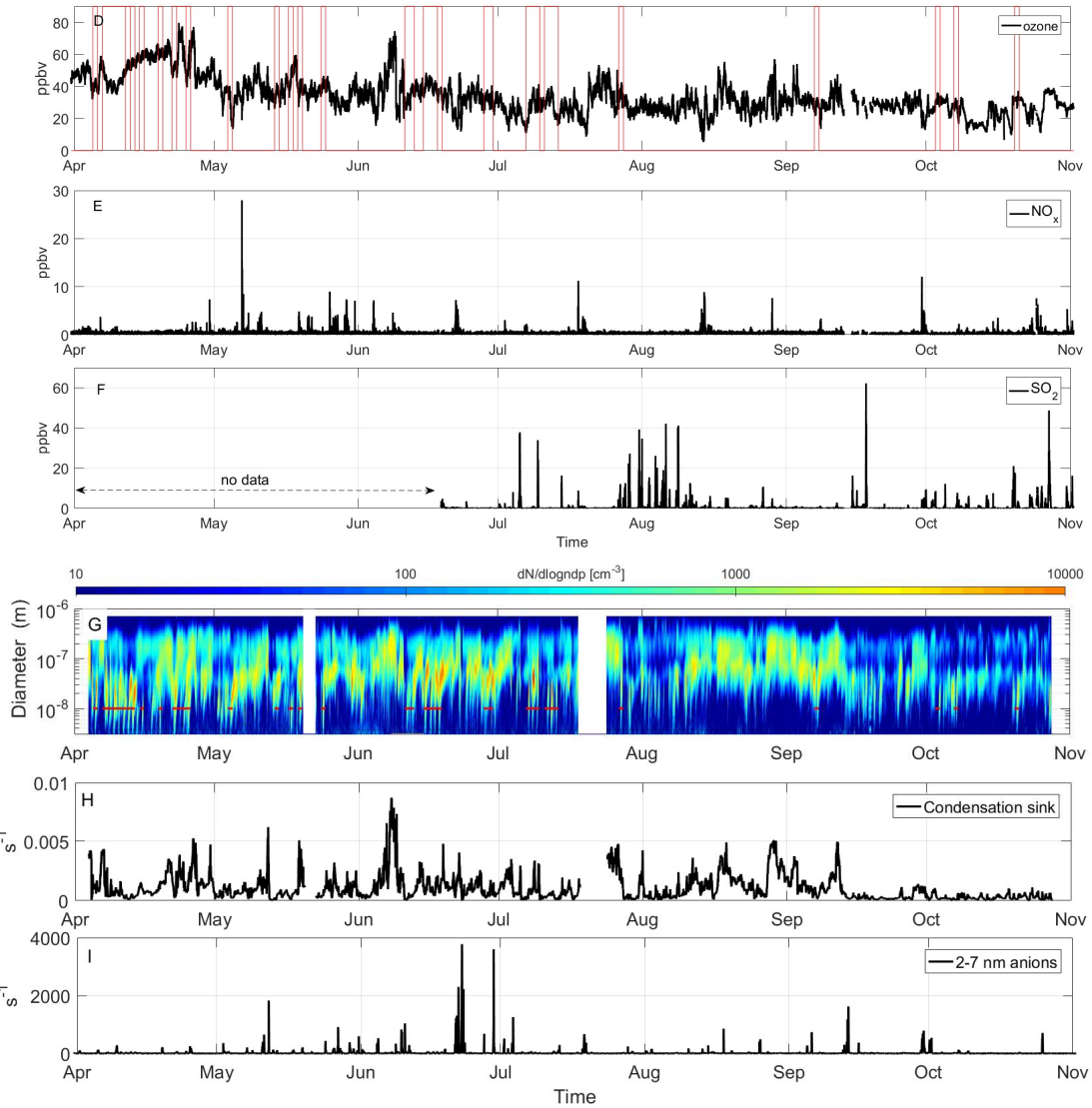
Figure 2: Observations of temperature (A), global radiation (B), snow depth (C), ozone (D), NOₓ (E) and SO₂ (F) mixing ratios, number size distribution (G), condensation sink (H) and concentration of 2-7 nm anions (I) at SMEAR I during the measurement period. SO₂ data is missing until mid-June due to instrumental malfunction. NPF event times are depicted in red in subplots (B), (D) and (G).

We can compare these numbers to SMEAR II long-term (5-year median concentration) observations, were the median peak SA concentrations are ~1.5 · 10^6 cm⁻³, ~1 · 10^6 cm⁻³ and ~3· 10^5 cm⁻³ for spring, summer and autumn, respectively (Sulo et al., 2021). These measured concentrations are very similar to SMEAR I observations except a slightly higher summer and autumn SA concentration at SMEAR II. However, it should be noted that the springtime measurements from SMEAR I do not include March data, which makes the springtime comparison somewhat uncertain. The SMEAR II data set that includes March data cannot be expected to be perfectly comparable with our data. However, as reported by Sipilä et al., 2021 the March data from the following year seems very similar concentration levels what we report in here for spring (max. ~2·10^6 cm⁻³ and daily averages peak around 0.5·10^6 cm⁻³). We expect that the SA concentrations are only marginally affected by the lack of March data, but that the level of HOMs or MSA or IA could be affected more due to very different meteorological conditions between the stations in springtime (SMEAR II is ~700 km more South than SMEAR I). There is also a difference in the timing of the peak SA concentration in the summer. At SMEAR I the peak concentration is reached at noon and at SMEAR II it can be found some hours earlier, already around eight o'clock in the morning (Sulo et al., 2021). In the case of HOMs, we cannot compare the concentrations directly to Sulo et al. (2021) as they calculated the sum of HOMs differently, only taking into account the most abundant signals and separating nitrate and non-nitrate HOMs. However, we take the liberty

to compare diurnal and seasonal variations. Both at SMEAR I and II, observations show the highest HOM concentrations during summer, while the autumn concentrations are one order of magnitude lower. The comparison between these sites reveals a different diurnal variation of HOMs. At SMEAR I, the HOMs have a maximum around noon, spanning to the afternoon (Figure 3). At SMEAR II, HOMs have two maxima, one at noon and another one in the early evening. From these, the latter is connected to non-nitrate monomer and dimer HOMs and nitrate dimer HOMs. At SMEAR I the lack of an evening maximum could indicate that HOM dimer formation is less dominant at SMEAR I compared to SMEAR II due to lower air temperatures, or due to the different diurnal cycle of oxidants due to longer hours of solar radiation North of the Arctic Circle.
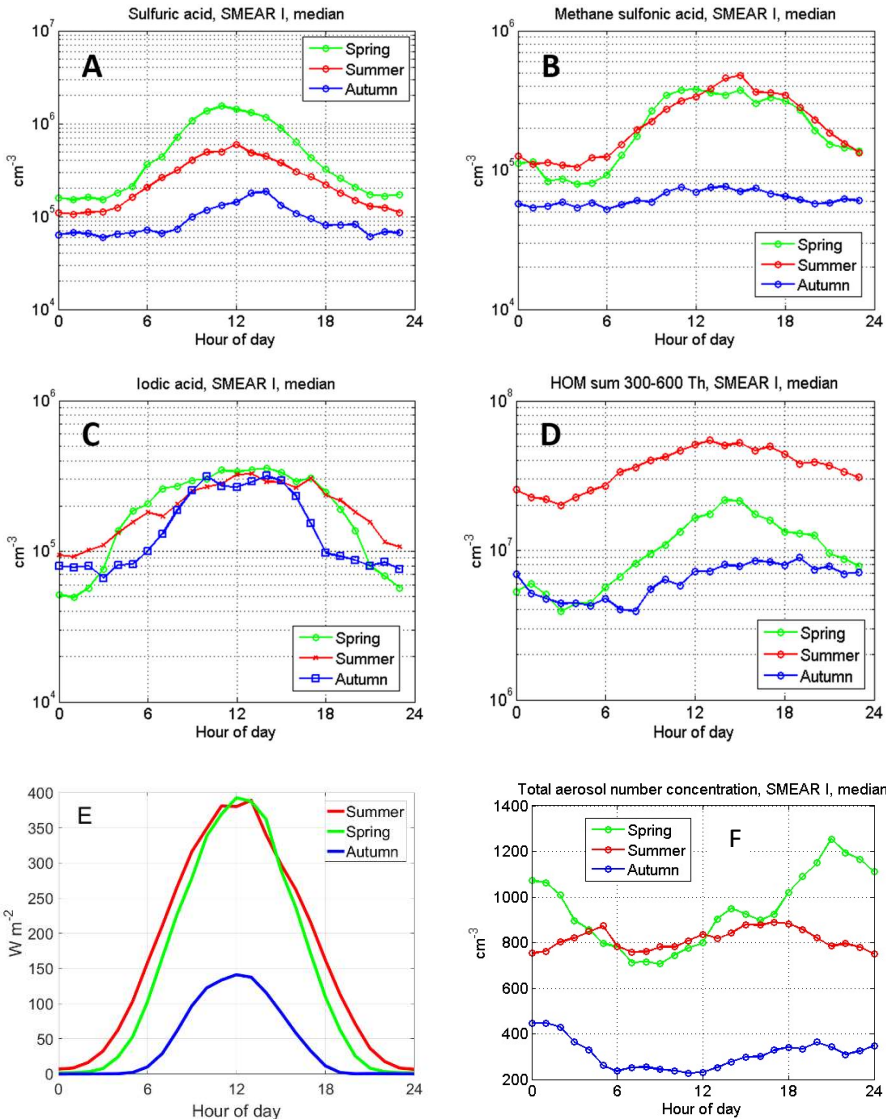
Figure 3. Diurnal variation of aerosol precursor gas median concentrations in different seasons: A) sulfuric acid, B) methane sulfonic acid, C) iodic acid and D) the sum of HOMs in the 300 to 600 Th mass range. Panel E) depicts the seasonal variation of global radiation and F) the total aerosol number concentration N_{tot}. The small (false) offset (6-7 W m^{-2}) in summer data is due to 24 h sunlight hours at Värriö.

When analyzing the monthly aerosol precursor profiles in Figure 4, we observe that the springtime atmosphere is abundant in SA and IA that have the highest median concentrations in April. MSA and HOMs concentrations peak in June. The MSA behavior is likely connected to the algae blooms in the Arctic Ocean that peak around midsummer. The marine emissions of DMS oxidize in the atmosphere to sulfur dioxide, SA and to MSA (e.g. Park et al., 2018). However, SA has more sources, since SO_2, has also anthropogenic sources. At SMEAR I

we cannot distinguish these sources precisely (more discussion about this in Sect 3.3.). It is notable that the peak concentration of MSA is earlier in the day in April, around 12 o'clock noon, than it is later in the year when the peak concentration is reached in the late afternoon (from 13:00 to 18:00 o'clock). There are no previous MSA concentration reports from the SMEAR stations but some gas phase MSA results from Antarctica show maximum of $1 \cdot 10^5$ cm^{-3} to $1 \cdot 10^7$ cm^{-3} concentrations (Jokinen et al., 2018; Mauldin et al., 2010, 2004). In the Arctic, around half a year measurement series from Villum in Greenland show MSA concentrations <10^6 cm^{-3} (Mar – Sep) and from 10^5 cm^{-3} to 10^7 cm^{-3} with the highest concentrations in June in Ny-Ålesund (Beck et al., 2021). Our measurements from the SMEAR I fall in between these extremes.
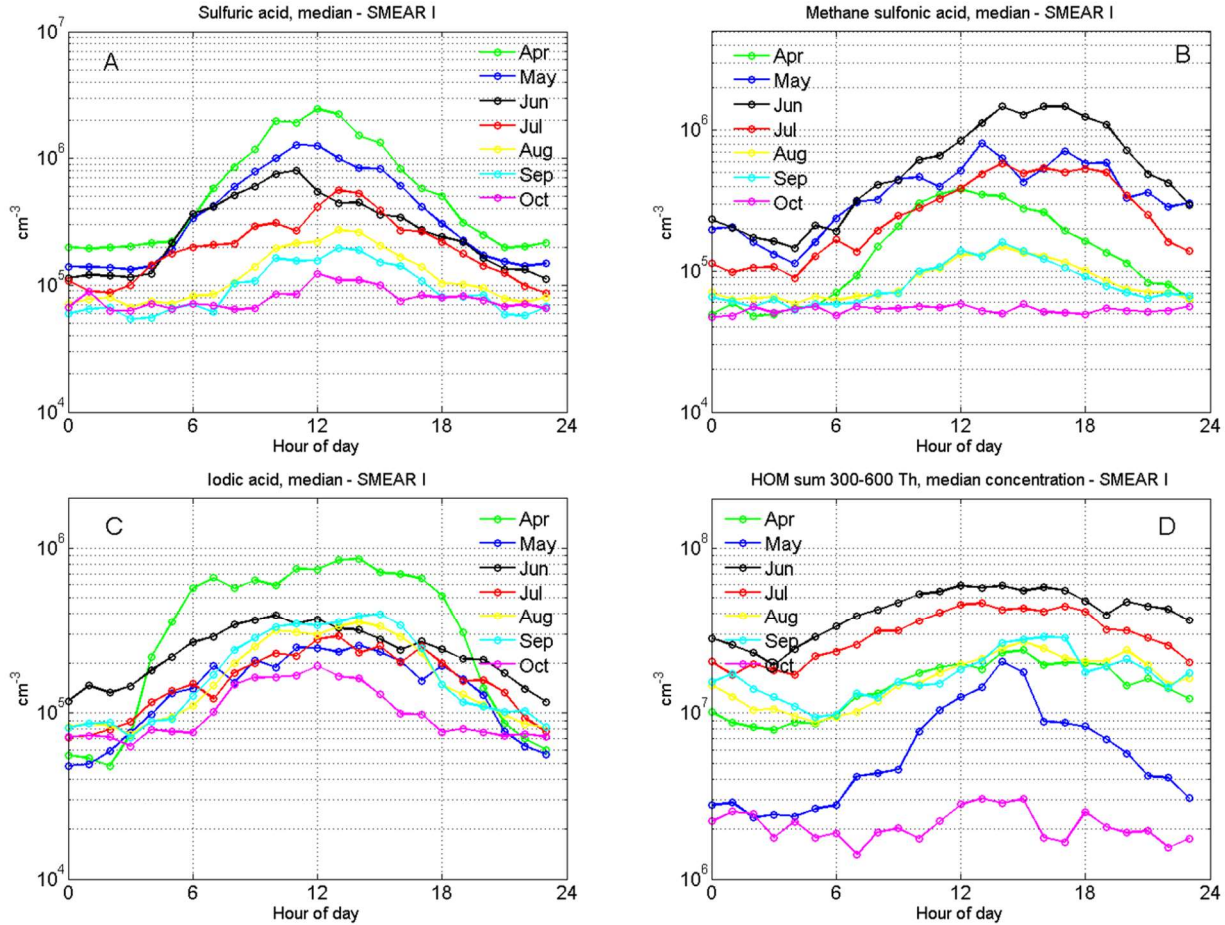
Figure 4. Monthly median concentrations of A) sulfuric acid, B) methane sulfonic acid, C) iodic acid and d) the sum of HOMs in the 300 to 600 Th mass range.

These are also the first reported results of IA measurements from SMEAR I and they represent a continental location, the White Sea coast being ~130 km South East and the Barents Sea ~230 km to the North East. IA, iodine and iodic oxoacid emissions are commonly connected to coastal or marine environments (Baccarini et al., 2020; McFiggans et al., 2010; O'dowd et al., 2002; Sipilä et al., 2016; Yu et al., 2019) due to the fact that the ocean surface is a major source of iodine (Carpenter et al., 2013). While it is not precisely known how IA forms in the gas phase, its formation requires oxidation of the initial precursors (IO$_x$ species) by ozone and the last steps of its formation is potentially driven by reaction with OH (Chameides and Davis, 1980).

Compared to the other precursor compounds, IA has the most stable concentration between seasons, with a long increasing period in April during the snow-melting season. This is likely due to the simultaneously increasing ozone mixing ratios (Figure 2D) and solar radiation. In contrast to measurements from the Arctic Ocean (Baccarini et al., 2020), we did not observe a clear increase in IA concentration in the autumn due to freezing. We find that September had only marginally higher concentrations compared to August or July

(Figure 4). Winter measurements would be necessary to estimate the effect of freezing in the concentration of IA.

The source of IA on a continental site like the SMEAR I is an interesting subject to speculate. The observed HIO_3 peak in April could indicate that there could be an influence from air masses exposed to Arctic marine environment. The increasing temperature in the spring induce a higher activity of phytoplankton in the nearby Barents Sea and Norwegian Sea that remains ice free, even during the winter, and could result in the higher emission of precursors for IA (Lai et al., 2011). Higher temperature would also result in more efficient advection, which would transport species faster from emission points to SMEAR I. The calculated back trajectories support the idea that iodine-rich air masses arrive from the West or northwest to SMEAR I (discussed in details in Sect 3.3. and Figure 10). This would be the hypothesis of the long-range transport for source of IA in SMEAR I. On the contrary, the strong diurnal variation on IA concentration seen as one order of magnitude difference between noon and midnight, suggests fast on-site chemistry, which is not consistent with long-range transport of IA, but its precursor such as CH_3I (Bell et al., 2002). Also, IA life time against condensational loss is expected to be short with the condensation sink at the site (Figure 2H), in the range of ~15 minutes, this suggests that HIO_3 is formed close to or at the site of measurements. Land vegetation is a source of methyl iodide (CH_3I) that could be the source of IA at SMEAR I at least during summer (Sive et al., 2007).

Most interestingly, we seem to have an emission source of iodine during all seasons. There are no reports on iodine emissions from continental snow, but we hypothesize that one possible source of iodine in SMEAR I during spring is the snowpack. This is possible due to the deposition of sea salts on snow particularly during dark periods that activate during the spring and are re-emitted to the atmosphere through heterogeneous photochemistry of iodide, and iodate ions (Raso et al., 2017; Spolaor et al., 2019). There are also possible forest emissions of iodinated organics, similar to New England growing season (Raso et al., 2017) that might be enhanced by higher temperature or high ozone concentrations. This type of emissions of iodinated gases, or their implications, have not been studied before but these observations might direct research into emission studies at SMEAR I, since our findings indicate that vegetation could be an emission source of iodine.

The sum of HOMs at SMEAR I reaches up to a median ~$5 \cdot 10^7$ cm^{-3} concentration in the summer. This is about one order of magnitude lower than the concentrations reported from the SMEAR II station in Hyytiälä (Yan et al., 2016) about 700 km south, where HOMs are at a maximum of ~$6 \cdot 10^8$ cm^{-3} during spring daytime. It is striking how well the concentration of HOMs follow the air temperature (Figure 5) but seem to level above circa 18°C. From the temperature dependency, we can speculate that most VOCs emitted by vegetation close to Värriö could be monoterpenes due to their strong temperature dependency. This is supported by emission rate measurements of VOCs showing that in northern Finland 60 to 85 % are accounted by α- and β-pinene emissions (Tarvainen et al., 2004). However, sesquiterpene emissions from nearby wetlands could contribute to HOMs since their emissions are also temperature dependent and they are emitted by the boreal wetlands (Hellén et al., 2020; Seco et al., 2020). As HOMs are oxidation products of VOCs, it is evident that the HOM concentration will increase in SMEAR I in the future with the increasing VOC emissions, including isoprene, monoterpenes and sesquiterpenes, due to temperature rise (Ghirardo et al., 2020; Tiiva et al., 2008; Valolahti et al., 2015).

337
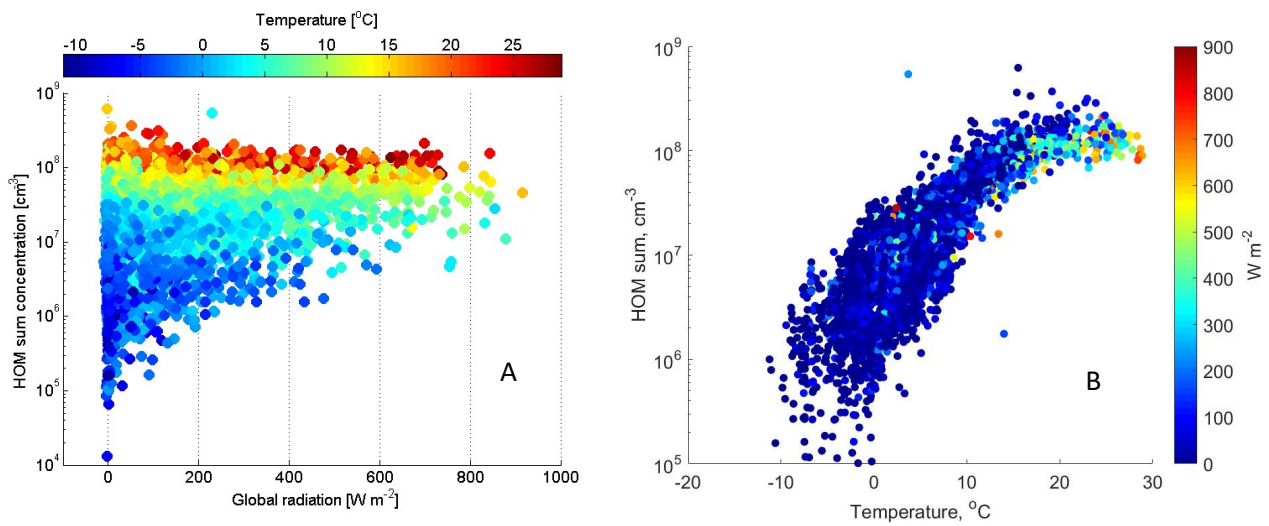
Figure 5. HOM concentration (cm^{-3}) measured at SMEAR I (sum of mass range from 300 to 600 Th) as a function of global radiation (W m^{-2}) in panel A and as a function of temperature in panel B. The color bar represents air temperature in °C (A) and global radiation (B). The plot includes all data measured from April to October 2019.

3.3. New particle formation events;

During the measurement period from 4 April 2019 to 27 October 2019, we observed 36 regional NPF events in total and our CI-APi-TOF data covers 33 of these NPF days. During the same period, we observed 75 non-event days without clear signs of particle formation (Maso et al., 2005). Rest of the days during our measurement period were defined as undefined, bad data or partly bad data days and these were excluded from our analysis. In this chapter, we focus on trace gases, meteorological parameters and detected aerosol precursor gases during NPF days and compare them to non-event days.

We plot NPF and non-event days median average number size distribution of aerosol particles (from 3 to 800 nm) in Figure 6, and the total number concentration and the 2-7 nm air ion concentrations in Figure 7. The whole measurement period is represented already in Figure 2. In figure 6, in the case of NPF event days we see a distinct "banana" plot, where small < 10 nm, particles are forming and growing with time. The DMPS data is plotted from 2.82 nm to 708 nm but note that the channels below ~5 nm have much larger uncertainties than those above. The median event start time is located around noon and the growth of particles continues steadily until midnight. However, when looking at individual days, there is a large variation in the start-times of the particle formation, some events start early in the morning or even in the night, while some start in late afternoon. Non-event days show very few particles in the < 10 nm size bins.

The total number of particles measured at the site during NPF events rises up to ~2400 cm^{-3} reaching the maximum concentration at ~17 o'clock in the evening. This shows that NPF is an important source of aerosol particles in Värriö as previously reported (Vehkamäki et al., 2004). Non-event days have clearly lower particle concentrations throughout the day, staying lower than 1000 cm^{-3} on average. The measured 2-7 nm anion concentrations stay very low during non-event days. As intermediate ions form mainly during NPF, their concentrations are used as indicator of NPF events in boreal environments (Leino et al., 2016). On NPF days, we see a peak in the anion concentration at noon, the concentration being about six times higher than during non-event days. This indicates that negative ions may play a role in SMEAR I particle formation events.
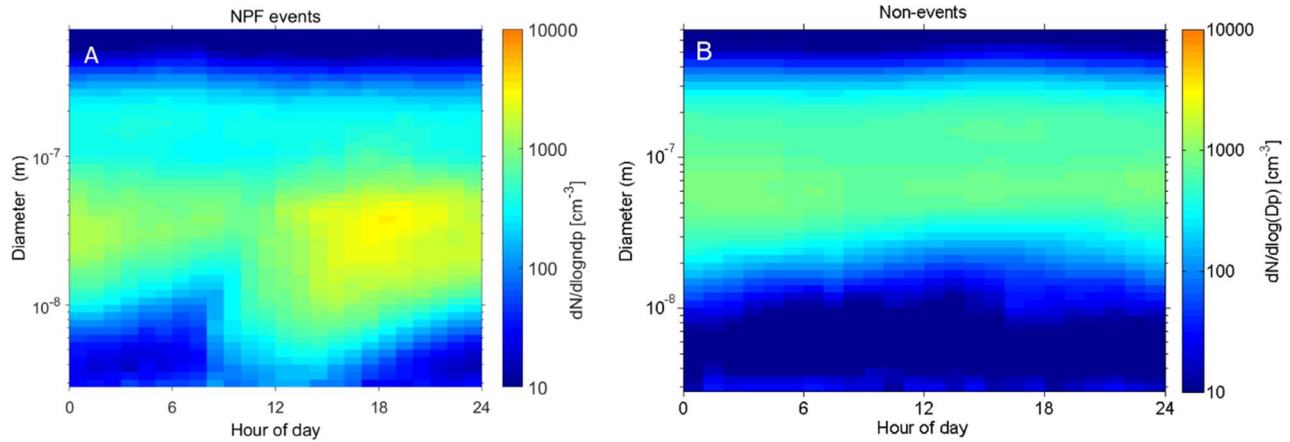
Figure 6. This figure depicts the median number size distribution during all observed NPF events (n = 33) and non-events (n = 75) during our measurement period. The data is collected with a DMPS and size bins from 2.82 to 708 nm are plotted.
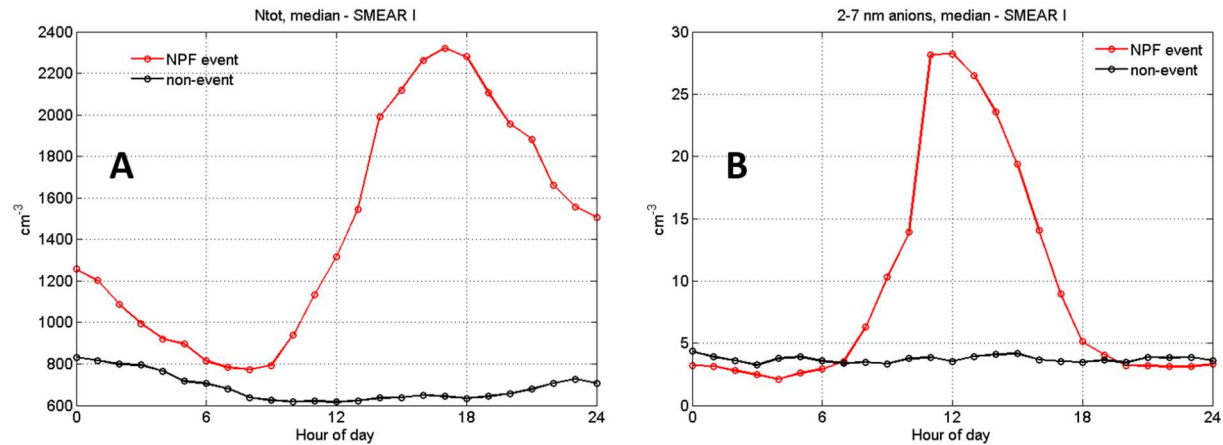
Figure 7. Median total particle concentration (N_{tot}) in A) and 2-7 nm negative ion concentrations in B) at SMEAR I during NPF event (red, n = 33) and non-event days (black, n = 75). The total particle number concentration is recorded with a CPC and air ion concentrations with a NAIS.

Figure 8 shows the differences in temperature, RH, global radiation and ozone mixing ratios between NPF event days (in red) and non-event days (black). In Värriö, NPF events preferably happen in relatively low temperatures (1 – 8 ˚C) with a fast temperature rise in the early morning hours, lower and decreasing RH, dropping from 90% to ~55 %, during the NPF days compared to non-event days. NPF days have clearly higher global irradiance values (~450 m⁻² vs. ~200 m⁻²) and about 10 ppbv higher ozone concentrations than non-event days. The meteorological conditions favor NPF are thus similar than at the SMEAR II station in Hyytiälä, where sunny clear sky days with low RH and condensation sink along with wind directions from the cleaner northerly sector are forecasting NPF events (Nieminen et al., 2014).

382
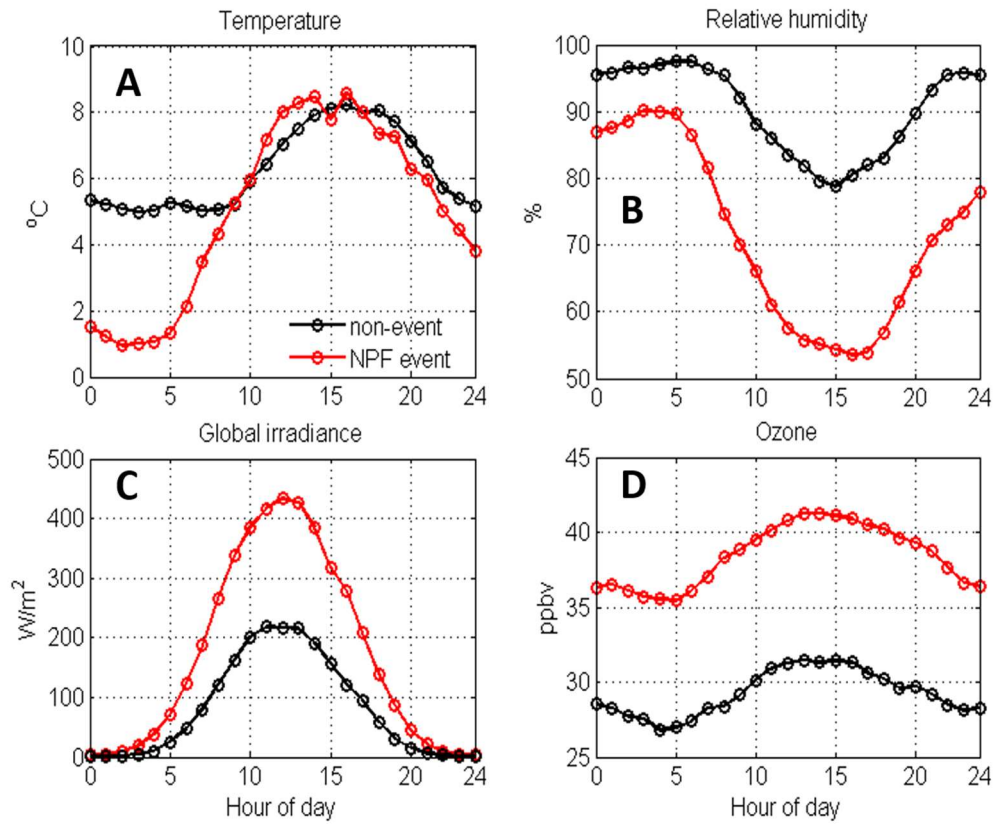
Figure 8. Average temperature (°C) in panel A), relative humidity (%) in B), global radiation (W m^{-2}) in C) and ozone concentration (ppbv) in D), all measured at SMEAR I during NPF event (red, n = 33) and non-event days (black, n = 75).

Next, we show the concentrations of aerosol precursor compounds during NPF and non-event days in figure 9. The SA concentrations closely follow the solar irradiation profile (Figure 8C). Similarly to the results obtained from the high Arctic, Svalbard, also MSA is elevated during NPF events, especially during summer, and could possibly contribute aerosol growth (Beck et al., 2021). We observe close to an order of magnitude higher MSA concentration between the events and non-events days, highlighting the dominant role of sulfur species to nucleation and growth in general at this site. In order to attribute the source of sulfur species and IA during the event and non-event days we performed a cluster analysis using a geographical information system (GIS) based software, Trajstat (Wang et al., 2009). The NCEP/NCAR reanalysis data was used as meteorological input for the model (Kalnay et al., 1996). The simulations were performed at an arrival height of 250 m. a.g.l. SMEAR I station is located approximately at similar height (390 m a.s.l), thus representing the air masses arriving at the station even during strong temperature inversions (Sipilä et al., 2021).

397
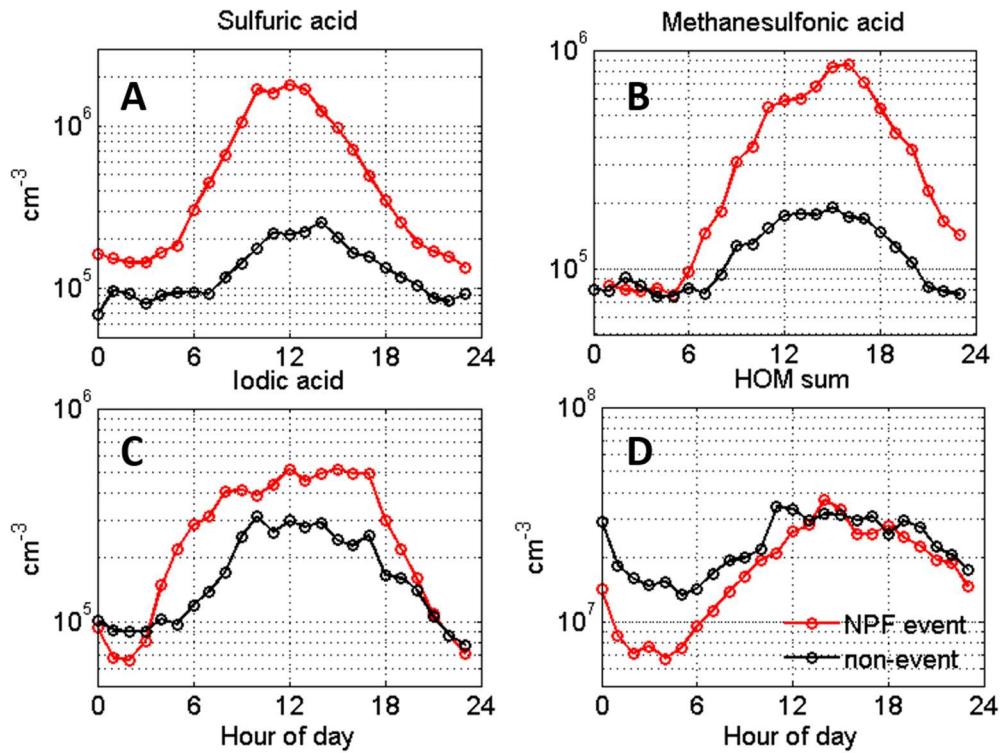
Figure 9. Aerosol precursor gases in SMEAR I during NPF (red, n = 33) and non-event days (black, n = 75). The data is hourly median average.

Higher concentrations of aerosol precursors SA, MSA and IA are connected to the air masses that arrive to SMEAR I from the Arctic Ocean (Figure 10). Cluster analysis of air mass back trajectories arriving to Värriö during NPF days clearly shows that most NPF events occur when the air mass was exposed to marine environments within the last 72 hours. In our case, mainly the Norwegian Sea in the West (58 %) or the Barents (21 %) and Kara Seas (21 %) in the Arctic Ocean. This seems relevant to our results since the marine environment in the North is emitting large amounts of DMS, a precursor for SA and MSA (Levasseur, 2013) and iodine species that further oxidize to IA (Baccarini et al., 2020; Sherwen et al., 2016). A fraction of air masses that are connected to both NPF (21 %) and non-event days (37 %) are coming to SMEAR I from the Kola peninsula that is connected to high SO_2 emissions, higher particle number concentrations and winter time NPF events (Sipilä et al., 2021). Most non-event air masses arrive to Värriö from South-West (49 %) crossing northern Finland and Sweden.

In addition from Figure 9 we observe that we cannot rule out the contribution of IA in NPF in SMEAR I, but with the recorded concentration, it usually is not enough to initiate NPF (He et al., 2021). Although IA concentrations are slightly larger on NPF days than non-event days, the rise in concentration happens already early in the morning, clearly before the average event start-time. The possible source of IA was discussed earlier in Sect 3.2 and we hypothesize that the source of iodine at SMEAR I could be both; i) the long distance transport from the Arctic Ocean combined to ii) the local emissions from the snow pack and vegetation. The hypothesis of vegetation emitted iodine species is supported by the minor difference between NPF (mostly marine) and non-event day (mostly continental) concentrations. At SMEAR I, HOMs are the only species that are at a (marginally) lower level during non-event than NPF days indicating that the total HOM concentration does not determine when NPF events occur. However, this does not exclude the possible participation of certain HOMs in NPF together with sulfur compounds (Lehtipalo et al., 2018) or at later stages of the NPF process, especially during particle growth. However, pure biogenic nucleation involving ions and HOMs (Kirkby et al., 2016) seems not to be a major NPF pathway in Värriö.

424 Our measurements do not unveil the detailed mechanism of nucleation or growth of particles. We lack
425 measurements of ambient bases that are needed to stabilize SA clusters in ambient conditions (e.g. Almeida et
426 al., 2013; Jen et al., 2014; Kirkby et al., 2011; Kürten et al., 2014; Myllys et al., 2018). With the given
427 observations comparing NPF days with non-event days it is likely that most regional NPF events require SA,
428 but the NPF process can involve other compounds as well, especially IA and MSA, which show higher
429 concentrations on NPF days, very similarly that the results reported from Ny-Ålesund (Beck et al., 2021).
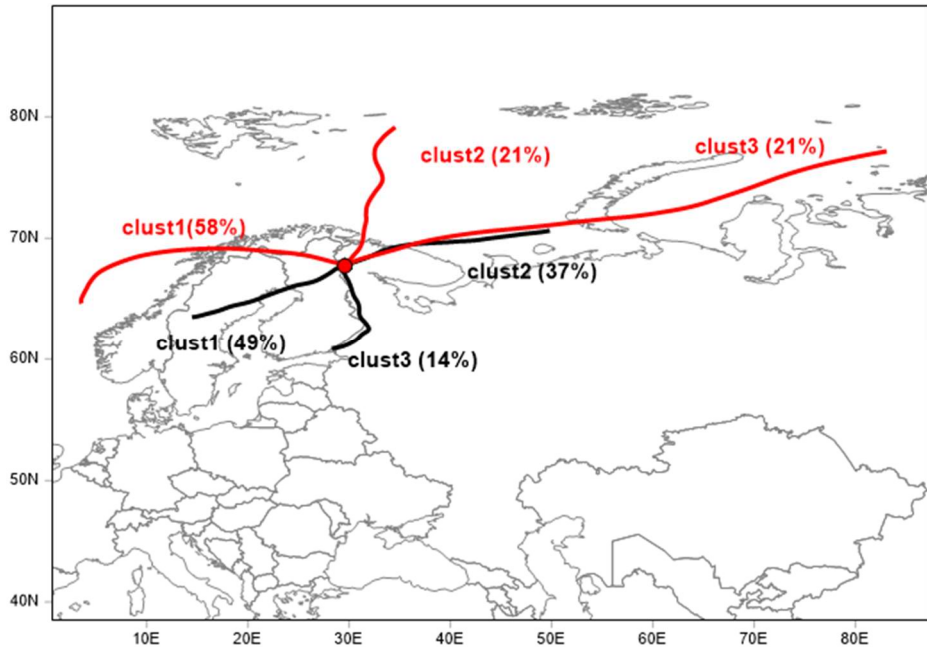
430

431 **Figure 10**. Trajectory cluster analysis of 72-hour back trajectories simulated at arrival height of 250 m a.g.l
432 and the NCEP/NCAR reanalysis data used as meteorological input. Red = NPF event, black = non-NPF

433 **4. Conclusions:**

434 We report ~7 months of nitrate-based CI-APi-TOF measurements of SA, MSA, IA and HOM from a remote
435 sub-Arctic field station SMEAR I in Finland. The measurements aim to increase our understanding of the
436 Arctic aerosol forming precursors and atmospheric chemistry in more details. The reason for measuring these
437 compounds ~150 km north of the Arctic Circle is simple; the Arctic is warming twice the speed as the planet
438 on average. Lapland is already facing environmental changes when e.g. woody plants disperse further north
439 and influence the tundra ecosystem (Aakala et al., 2014; Kemppinen et al., 2021). These changes will in turn
440 affect the emissions of aerosol precursor gases, which may have feedback effects on to the climate (e.g.
441 Kulmala et al., 2020; Paasonen et al., 2013).

442 The area surrounding SMEAR I station has snow cover for almost 8 months a year. Accumulating snow during
443 the autumn is a good reservoir to e.g. halogens, similarly than in the high Arctic (and Arctic Ocean)
444 environment. The snow pack also acts as a cover for biogenic emissions entering the atmosphere from the
445 ground. Any changes in the temperature and snow cover in the sub-Arctic regions will effect on atmospheric
446 chemistry and composition that are undeniably changing the way aerosol particles form and what their number
447 concentration is in the region.

448 In this study, we report seasonal and monthly variations of SA, MSA, IA and HOM concentrations and find
449 all these compounds abundant in springtime. SA has a peak concentration in the spring, decreasing for the rest
450 of the seasons. We detect high concentrations of MSA and IA that are usually connected to marine and coastal
451 environments, although Värriö is located ~130 km from the nearest coast of the White Sea. While MSA is
452 abundant in the spring, summer and decreases to limit of detection levels for autumn, IA continues at the same

concentration throughout the seasons. It seems likely that these two compounds are connected to emissions from phytoplankton or the Arctic ice pack and arrive to SMEAR I by long transport routes. In the case of IA, we suggest that the source of iodine emissions is a combination of transport and local emission from the continental snow pack and vegetation at the site. Further work is needed to confirm this hypothesis.

The most striking correlation we found in HOM concentrations and ambient air temperature. The vegetation at SMEAR I is the source of VOCs even in the snow covered spring season and these volatile gases are oxidized into HOMs with different reaction rates depending on the oxidant. In the case of such strong temperature controlled HOM concentrations, we conclude that HOMs in the mass range of 300 – 600 Th are most likely products of monoterpene oxidation.

We also studied the abundance of these aerosol precursors separately during NPF and non-event days. We observed that new particles at SMEAR I preferably form in relatively low temperatures (< 10°C), low RH that decreases with rising temperature during the day (to a minimum of ~55%), ~10 ppbv higher ozone mixing ratio than during non-event days, high SA concentration in the morning and high MSA concentrations in the afternoon. Cluster analysis of air masses show that NPF usually happens in marine air masses travelling to the site from North West – West. All together, these are the first long term measurements of aerosol forming precursor from the sub-arctic region helping us to understand atmospheric chemical processes and aerosol formation in the rapidly changing Arctic.

Data availability:

All meteorological parameters, trace gas concentrations and aerosol data we downloaded directly from smartSMEAR open access database (https://smear.avaa.csc.fi/). Mass spectrometric data, event analysis, condensation sink and anion concentration data are available on Zenodo, https://doi.org/10.5281/zenodo.5879549.

Author contribution:

TJ, MS, TP and MK designed the experiments at SMEAR I and MS, NS, KN and TL carried them out. IY made the NPF event analysis and RT calculated the back trajectories. TJ and KL wrote the manuscript with contributions from all co-authors.

Competing interests:

Markku Kulmala is editor of ACP. Tuukka Petäjä is editor of ACP.

Acknowledgements:

We would like to thank the technical staff in Kumpula and Värriö, who keep the long-term measurements going and helped with data collection, instrument calibrations, logistics and in data quality control and assurance during the year. We acknowledge the important role our collaborators have in scientific discussion and a special thanks goes to Alfonso Saiz-Lopez for IA related discussion that helped to draft this article. We thank the ACTRIS CiGas-UHEL unit for mass spectrometer calibration support and the tofTools team for data analysis software.

Financial support:

The Academy of Finland via Center of Excellence in Atmospheric Sciences (project no. 272041) and European Research Council via ATM-GTP 266 (742206), GASPARCON (714621) and Flagship funding (grant no. 337549) funded this work. We also received funding from the Academy of Finland (project no. 1235656, 296628, 316114, 315203, 307537, 325647, 33397, 334792 and 334514) "Quantifying carbon sink, CarbonSink+ and their interaction with air quality" and Academy professorship (grant no. 302958). This work was further supported by the European Commission via via project iCUPE (Integrative and Comprehensive Understanding on Polar Environments, No 689443), the EMME-CARE project which received funding from the European Union's Horizon 2020 Research and Innovation Programme, under grant agreement no. 856612,

Regional Council of Lapland (Värriön tutkimusaseman huipputhutkimus hyödyntämään Itä-Lapin elinkeinoelämää, VÄRI, A74190) and Aatos Erkko Foundation.

References:

Aakala, T., Hari, P., Dengel, S., Newberry, S. L., Mizunuma, T. and Grace, J.: A prominent stepwise advance of the tree line in north-east Finland, J. Ecol., 102(6), 1582–1591, doi:10.1111/1365-2745.12308, 2014.

Ahonen, T., Aalto, P., Rannik, Ü., Kulmala, M., Nilsson, E. D., Palmroth, S., Ylitalo, H. and Hari, P.: Variations and vertical profiles of trace gas and aerosol concentrations and CO2 exchange in eastern Lapland, Atmos. Environ., 31(20), 3351–3362, doi:10.1016/S1352-2310(97)00151-9, 1997.

Almeida, J., Schobesberger, S., Kürten, A., Ortega, I. K., Kupiainen-Määttä, O., Praplan, A. P., Adamov, A., Amorim, A., Bianchi, F., Breitenlechner, M., David, A., Dommen, J., Donahue, N. M., Downard, A., Dunne, E., Duplissy, J., Ehrhart, S., Flagan, R. C., Franchin, A., Guida, R., Hakala, J., Hansel, A., Heinritzi, M., Henschel, H., Jokinen, T., Junninen, H., Kajos, M., Kangasluoma, J., Keskinen, H., Kupc, A., Kurtén, T., Kvashin, A. N., Laaksonen, A., Lehtipalo, K., Leiminger, M., Leppä, J., Loukonen, V., Makhmutov, V., Mathot, S., McGrath, M. J., Nieminen, T., Olenius, T., Onnela, A., Petäjä, T., Riccobono, F., Riipinen, I., Rissanen, M., Rondo, L., Ruuskanen, T., Santos, F. D., Sarnela, N., Schallhart, S., Schnitzhofer, R., Seinfeld, J. H., Simon, M., Sipilä, M., Stozhkov, Y., Stratmann, F., Tomé, A., Tröstl, J., Tsagkogeorgas, G., Vaattovaara, P., Viisanen, Y., Virtanen, A., Vrtala, A., Wagner, P. E., Weingartner, E., Wex, H., Williamson, C., Wimmer, D., Ye, P., Yli-Juuti, T., Carslaw, K. S., Kulmala, M., Curtius, J., Baltensperger, U., Worsnop, D. R., Vehkamäki, H. and Kirkby, J.: Molecular understanding of sulphuric acid-amine particle nucleation in the atmosphere, Nature, 502(7471), 359–363, doi:10.1038/nature12663, 2013.

Baccarini, A., Karlsson, L., Dommen, J., Duplessis, P., Vüllers, J., Brooks, I. M., Saiz-Lopez, A., Salter, M., Tjernström, M., Baltensperger, U., Zieger, P. and Schmale, J.: Frequent new particle formation over the high Arctic pack ice by enhanced iodine emissions, Nat. Commun., 11(1), doi:10.1038/s41467-020-18551-0, 2020.

Beck, L. J., Sarnela, N., Junninen, H., Hoppe, C. J. M. M., Garmash, O., Bianchi, F., Riva, M., Rose, C., Peräkylä, O., Wimmer, D., Kausiala, O., Jokinen, T., Ahonen, L., Mikkilä, J., Hakala, J. J., He, X.-C. C., Kontkanen, J., Wolf, K. K. E. E., Cappelletti, D., Mazzola, M., Traversi, R., Petroselli, C., Viola, A. P., Vitale, V., Lange, R., Massling, A., Nøjgaard, J. K., Krejci, R., Karlsson, L., Zieger, P., Jang, S. S., Lee, K., Vakkari, V., Lampilahti, J., Thakur, R. C., Leino, K., Kangasluoma, J., Duplissy, E.-M. M., Siivola, E., Marbouti, M., Tham, Y. J., Saiz-Lopez, A., Petäjä, T., Ehn, M., Worsnop, D. R., Skov, H., Kulmala, M., Kerminen, V.-M. M., Sipilä, M., Nojgaard, J., Krejci, R., Karlsson, L., Zieger, P., Jang, S. S., Lee, K., Vakkari, V., Lampilahti, J., Thakur, R. C., Leino, K., Kangasluoma, J., Duplissy, E.-M. M., Siivola, E., Marbouti, M., Tham, Y. J., Saiz-Lopez, A., Petäjä, T., Ehn, M., Worsnop, D. R., Skov, H., Kulmala, M., Kerminen, V.-M. M. and Sipilä, M.: Differing Mechanisms of New Particle Formation at Two Arctic Sites, Geophys. Res. Lett., 48(4), e2020GL091334, doi:10.1029/2020GL091334, 2021.

Bell, N., Hsu, L., Jacob, D. J., Schultz, M. G., Blake, D. R., Butler, J. H., King, D. B., Lobert, J. M. and Maier-Reimer, E.: Methyl iodide: Atmospheric budget and use as a tracer of marine convection in global models, J. Geophys. Res. Atmos., 107(D17), ACH 8-1, doi:10.1029/2001JD001151, 2002.

Berndt, T., Richters, S., Jokinen, T., Hyttinen, N., Kurtén, T., Otkjær, R. V., Kjaergaard, H. G., Stratmann, F., Herrmann, H., Sipilä, M., Kulmala, M. and Ehn, M.: Hydroxyl radical-induced formation of highly oxidized organic compounds, Nat. Commun., 7, 13677, doi:10.1038/ncomms13677, 2016.

Bianchi, F., Garmash, O., He, X., Yan, C., Iyer, S., Rosendahl, I., Xu, Z., Rissanen, M. P., Riva, M., Taipale, R., Sarnela, N., Petäjä, T., Worsnop, D. R., Kulmala, M., Ehn, M. and Junninen, H.: The role of highly oxygenated molecules (HOMs) in determining the composition of ambient ions in the boreal forest, Atmos. Chem. Phys., 17(22), 13819–13831, doi:10.5194/acp-17-13819-2017, 2017.

Bradshaw, C. J. A. and Warkentin, I. G.: Global estimates of boreal forest carbon stocks and flux, Glob. Planet. Change, 128, 24–30, doi:10.1016/j.gloplacha.2015.02.004, 2015.

Brandt, J. P., Flannigan, M. D., Maynard, D. G., Thompson, I. D. and Volney, W. J. A.: An introduction to Canada's boreal zone: Ecosystem processes, health, sustainability, and environmental issues1, Environ. Rev., 21(4), 207–226, doi:10.1139/er-2013-0040, 2013.

Carpenter, L. J., MacDonald, S. M., Shaw, M. D., Kumar, R., Saunders, R. W., Parthipan, R., Wilson, J. and Plane, J. M. C.: Atmospheric iodine levels influenced by sea surface emissions of inorganic iodine, Nat. Geosci., 6(2), 108–111, doi:10.1038/ngeo1687, 2013.

Chameides, W. L. and Davis, D. D.: Iodine: Its possible role in tropospheric photochemistry, J. Geophys. Res. Ocean., 85(C12), 7383–7398, doi:10.1029/JC085IC12P07383, 1980.

Charlson, R. J., Lovelock, J. E., Andreae, M. O. and Warren, S. G.: Oceanic phytoplankton, atmospheric sulphur, cloud albedo and climate, Nature, 326(6114), 655–661, doi:10.1038/326655a0, 1987.

Dal Maso, M., Sogacheva, L., Aalto, P. P., Riipinen, I., Komppula, M., Tunved, P., Korhonen, L., Suur-Uski, V., Hirsikko, A., KurtéN, T., Kerminen, V.-M. M., Lihavainen, H., Viisanen, Y. Y., Hansson, H.-C. C., Kulmala, M., Maso, M. D., Sogacheva, L., Aalto, P. P., Riipinen, I., Komppula, M., Tunved, P., Korhonen, L., Suur-Uski, V., Hirsikko, A., KurtéN, T., Kerminen, V.-M. M., Lihavainen, H., Viisanen, Y. Y., Hansson, H.-C. C., Kulmala, M., Dal Maso, M., Sogacheva, L., Aalto, P. P., Riipinen, I., Komppula, M., Tunved, P., Korhonen, L., Suur-Uski, V., Hirsikko, A., KurtéN, T., Kerminen, V.-M. M., Lihavainen, H., Viisanen, Y. Y., Hansson, H.-C. C., Kulmala, M.: Aerosol size distribution measurements at four Nordic field stations: Identification, analysis and trajectory analysis of new particle formation bursts, Tellus, Ser. B Chem. Phys. Meteorol., 59(3), 350–361, doi:10.1111/j.1600-0889.2007.00267.x, 2007.

Dall Osto, M., Geels, C., Beddows, D. C. S., Boertmann, D., Lange, R., Nøjgaard, J. K., Harrison, R. M., Simo, R., Skov, H. and Massling, A.: Regions of open water and melting sea ice drive new particle formation in North East Greenland., Sci. Rep., 8(1), 6109, doi:10.1038/s41598-018-24426-8, 2018.

Ehn, M., Thornton, J. A., Kleist, E., Sipilä, M., Junninen, H., Pullinen, I., Springer, M., Rubach, F., Tillmann, R., Lee, B., Lopez-Hilfiker, F., Andres, S., Acir, I.-H. H., Rissanen, M., Jokinen, T., Schobesberger, S., Kangasluoma, J., Kontkanen, J., Nieminen, T., Kurtén, T., Nielsen, L. B., Jørgensen, S., Kjaergaard, H. G., Canagaratna, M., Maso, M. D., Berndt, T., Petäjä, T., Wahner, A., Kerminen, V.-M. M., Kulmala, M., Worsnop, D. R., Wildt, J. and Mentel, T. F.: A large source of low-volatility secondary organic aerosol, Nature, 506(7489), 476–479, doi:10.1038/nature13032, 2014.

Ghirardo, A., Lindstein, F., Koch, K., Buegger, F., Schloter, M., Albert, A., Michelsen, A., Winkler, J. B., Schnitzler, J.-P. and Rinnan, R.: Origin of volatile organic compound emissions from subarctic tundra under global warming, Glob. Chang. Biol., 26(3), 1908–1925, doi:10.1111/GCB.14935, 2020.

Hari, P., Aalto, P., Hämeri, K., Kulmala, M., Lahti, T., Luoma, S., Palva, L., Pohja, T., Pulliainen, E., Siivola, E. and Vesala, T.: Air pollution in eastern Lapland: challenge for an environmental measurement station, Silva Fenn., 28(1), 29–39, doi:10.14214/SF.A9160, 1994.

He, X.-C., Tham, Y. J., Dada, L., Wang, M., Finkenzeller, H., Stolzenburg, D., Iyer, S., Simon, M., Kürten, A., Shen, J., Rörup, B., Rissanen, M., Schobesberger, S., Baalbaki, R., Wang, D. S., Koenig, T. K., Jokinen, T., Sarnela, N., Beck, L. J., Almeida, J., Amanatidis, S., Amorim, A., Ataei, F., Baccarini, A., Bertozzi, B., Bianchi, F., Brilke, S., Caudillo, L., Chen, D., Chiu, R., Chu, B., Dias, A., Ding, A., Dommen, J., Duplissy, J., Haddad, I. El, Carracedo, L. G., Granzin, M., Hansel, A., Heinritzi, M., Hofbauer, V., Junninen, H., Kangasluoma, J., Kemppainen, D., Kim, C., Kong, W., Krechmer, J. E., Kvashin, A., Laitinen, T., Lamkaddam, H., Lee, C. P., Lehtipalo, K., Leiminger, M., Li, Z., Makhmutov, V., Manninen, H. E., Marie, G., Marten, R., Mathot, S., Mauldin, R. L., Mentler, B., Möhler, O., Müller, T., Nie, W., Onnela, A., Petäjä, T., Pfeifer, J., Philippov, M., Ranjithkumar, A., Saiz-Lopez, A., Salma, I., Scholz, W., Schuchmann, S., Schulze, B., Steiner, G., Stozhkov, Y., Tauber, C., Tomé, A., Thakur, R. C., Väisänen, O., Vazquez-Pufleau, M., Wagner, A. C., Wang, Y., Weber, S. K., Winkler, P. M., Wu, Y., Xiao, M., Yan, C., Ye, Q., Ylisirniö, A., Zauner-Wieczorek, M., Zha, Q., Zhou, P., Flagan, R. C., Curtius, J., Baltensperger, U., Kulmala, M., Kerminen, V.-M., Kurtén, T., et al.: Role of iodine oxoacids in atmospheric aerosol nucleation, Science (80-.)., 371(6529), 589–595, doi:10.1126/SCIENCE.ABE0298, 2021.

Hellén, H., Schallhart, S., Praplan, A., Tykkä, T., Aurela, M., Lohila, A. and Hakola, H.: Terpenoid

measurements at a Northern wetland revealed a strong source of sesquiterpenes, Atmos. Chem. Phys. Discuss., 1–20, doi:10.5194/ACP-2019-1154, 2020.

Hyttinen, N., Kupiainen-Määttä, O., Rissanen, M. P., Muuronen, M., Ehn, M. and Kurtén, T.: Modeling the Charging of Highly Oxidized Cyclohexene Ozonolysis Products Using Nitrate-Based Chemical Ionization, J. Phys. Chem. A, 119(24), 6339–6345, 2015.

IPCC, F. assessment report: Fifth Assessment Report - Climate Change 2013, IPCC, Fifth Assess. Rep. - Clim. Chang. [online] Available from: http://www.ipcc.ch/report/ar5/wg1/, 2013.

Jen, C. N., McMurry, P. H. and Hanson, D. R.: Stabilization of sulfuric acid dimers by ammonia, methylamine, dimethylamine, and trimethylamine, J. Geophys. Res. Atmos., 119(12), 7502–7514, doi:10.1002/2014JD021592, 2014.

Jokinen, T., Sipilä, M., Junninen, H., Ehn, M., Lönn, G., Hakala, J., Petäjä, T., Mauldin, R. L., Kulmala, M. and Worsnop, D. R.: Atmospheric sulphuric acid and neutral cluster measurements using CI-APi-TOF, Atmos. Chem. Phys., 12(9), 4117–4125, doi:10.5194/acp-12-4117-2012, 2012.

Jokinen, T., Sipilä, M., Richters, S., Kerminen, V.-M. M., Paasonen, P., Stratmann, F., Worsnop, D., Kulmala, M., Ehn, M., Herrmann, H. and Berndt, T.: Rapid autoxidation forms highly oxidized RO2 radicals in the atmosphere, Angew. Chemie Int. Ed., 53(52), 14596–14600, doi:10.1002/anie.201408566, 2014.

Jokinen, T., Kontkanen, J., Lehtipalo, K., Manninen, H. E., Aalto, J., Porcar-Castell, A., Garmash, O., Nieminen, T., Ehn, M., Kangasluoma, J., Junninen, H., Levula, J., Duplissy, J., Ahonen, L. R., Rantala, P., Heikkinen, L., Yan, C., Sipilä, M., Worsnop, D. R., Bäck, J., Petäjä, T., Kerminen, V.-M. and Kulmala, M.: Solar eclipse demonstrating the importance of photochemistry in new particle formation., Sci. Rep., 7, 45707, doi:10.1038/srep45707, 2017.

Jokinen, T., Sipilä, M., Kontkanen, J., Vakkari, V., Tisler, P., Duplissy, E. M., Junninen, H., Kangasluoma, J., Manninen, H. E., Petäjä, T., Kulmala, M., Worsnop, D. R., Kirkby, J., Virkkula, A. and Kerminen, V. M.: Ion-induced sulfuric acid–ammonia nucleation drives particle formation in coastal Antarctica, , 4(11), eaat9744, doi:10.1126/SCIADV.AAT9744, 2018.

Junninen, H., Ehn, M., Petäjä, T., Luosujärvi, L., Kotiaho, T., Kostiainen, R., Rohner, U., Gonin, M., Fuhrer, K., Kulmala, M. and Worsnop, D. R.: A high-resolution mass spectrometer to measure atmospheric ion composition, Atmos. Meas. Tech., 3(4), 1039–1053, doi:10.5194/amt-3-1039-2010, 2010.

Kalnay, E., Kanamitsu, M., Kistler, R., Collins, W., Deaven, D., Gandin, L. and E. Kalnay M. Kanamitsu R. Kistler W. Collins D. Deaven L. Gandin M. Iredell S. Saha G. White J. Woollen Y. Zhu M. Chelliah W. Ebisuzaki W. HE. Kalnay M. Kanamitsu R. Kistler W. Collins D. Deaven L. Gandin M. Iredell S. Saha G. White, and D. J.: The NCEP/NCAR 40-Year Reanalysis Project, Bull. Am. Meteorol. Soc., 437–472, doi:https://doi.org/10.1175/1520-0477(1996)077<0437:TNYRP>2.0.CO;2, 1996.

Kemppinen, J., Niittynen, P., Virkkala, A.-M., Happonen, K., Riihimäki, H., Aalto, J. and Luoto, M.: Dwarf Shrubs Impact Tundra Soils: Drier, Colder, and Less Organic Carbon, Ecosyst. 2021, 1–15, doi:10.1007/S10021-020-00589-2, 2021.

Kerminen, V.-M., Paramonov, M., Anttila, T., Riipinen, I., Fountoukis, C., Korhonen, H., Asmi, E., Laakso, L., Lihavainen, H., Swietlicki, E., Svenningsson, B., Asmi, A., Pandis, S. N., Kulmala, M. and Petäjä, T.: Cloud condensation nuclei production associated with atmospheric nucleation: a synthesis based on existing literature and new results, Atmos. Chem. Phys., 12(24), 12037–12059, doi:10.5194/acp-12-12037-2012, 2012.

Kerminen, V., Aurela, M., Hillamo, R. E. and Virkkula, A.: Formation of particulate MSA: deductions from size distribution measurements in the Finnish Arctic, Tellus B, 49(2), 159–171, doi:10.1034/j.1600-0889.49.issue2.4.x, 1997.

Kirkby, J., Curtius, J., Almeida, J., Dunne, E., Duplissy, J., Ehrhart, S., Franchin, A., Gagné, S., Ickes, L., Kürten, A., Kupc, A., Metzger, A., Riccobono, F., Rondo, L., Schobesberger, S., Tsagkogeorgas, G., Wimmer, D., Amorim, A., Bianchi, F., Breitenlechner, M., David, A., Dommen, J., Downard, A., Ehn, M.,

Flagan, R. C., Haider, S., Hansel, A., Hauser, D., Jud, W., Junninen, H., Kreissl, F., Kvashin, A., Laaksonen, A., Lehtipalo, K., Lima, J., Lovejoy, E. R., Makhmutov, V., Mathot, S., Mikkilä, J., Minginette, P., Mogo, S., Nieminen, T., Onnela, A., Pereira, P., Petäjä, T., Schnitzhofer, R., Seinfeld, J. H., Sipilä, M., Stozhkov, Y., Stratmann, F., Tomé, A., Vanhanen, J., Viisanen, Y., Vrtala, A., Wagner, P. E., Walther, H., Weingartner, E., Wex, H., Winkler, P. M., Carslaw, K. S., Worsnop, D. R., Baltensperger, U. and Kulmala, M.: Role of sulphuric acid, ammonia and galactic cosmic rays in atmospheric aerosol nucleation., Nature, 476(7361), 429–433, doi:10.1038/nature10343, 2011.

Kirkby, J., Duplissy, J., Sengupta, K., Frege, C., Gordon, H., Williamson, C., Heinritzi, M., Simon, M., Yan, C., Almeida, J. J., Trostl, J., Nieminen, T., Ortega, I. K., Wagner, R., Adamov, A., Amorim, A., Bernhammer, A.-K. K., Bianchi, F., Breitenlechner, M., Brilke, S., Chen, X., Craven, J., Dias, A., Ehrhart, S., Flagan, R. C., Franchin, A., Fuchs, C., Guida, R., Hakala, J., Hoyle, C. R., Jokinen, T., Junninen, H., Kangasluoma, J., Kim, J., Krapf, M., Kurten, A., Laaksonen, A., Lehtipalo, K., Makhmutov, V., Mathot, S., Molteni, U., Onnela, A., Perakyla, O., Piel, F., Petaja, T., Praplan, A. P., Pringle, K., Rap, A., Richards, N. A. D. D., Riipinen, I., Rissanen, M. P., Rondo, L., Sarnela, N., Schobesberger, S., Scott, C. E., Seinfeld, J. H., Sipila, M., Steiner, G., Stozhkov, Y., Stratmann, F., Tomé, A., Virtanen, A., Vogel, A. L., Wagner, A. C., Wagner, P. E., Weingartner, E., Wimmer, D., Winkler, P. M., Ye, P., Zhang, X., Hansel, A., Dommen, J., Donahue, N. M., Worsnop, D. R., Baltensperger, U., Kulmala, M., Carslaw, K. S., Curtius, J., Tröstl, J., Nieminen, T., Ortega, I. K., Wagner, R., Adamov, A., Amorim, A., Bernhammer, A.-K. K., Bianchi, F., Breitenlechner, M., Brilke, S., Chen, X., Craven, J., Dias, A., Ehrhart, S., Flagan, R. C., Franchin, A., Fuchs, C., Guida, R., Hakala, J., Hoyle, C. R., Jokinen, T., et al.: Ion-induced nucleation of pure biogenic particles, Nature, 533(7604), 521–526, doi:10.1038/nature17953, 2016.

Kulmala, M., Toivonen, A., Mäkelä, J. M. and Laaksonen, A.: Analysis of the growth of nucleation mode particles observed in Boreal forest, Tellus B, 50(5), 449–462, doi:10.1034/j.1600-0889.1998.t01-4-00004.x, 1998.

Kulmala, M., Riipinen, I., Sipilä, M., Manninen, H. E., Petäjä, T., Junninen, H., Dal Maso, M., Mordas, G., Mirme, A., Vana, M., Hirsikko, A., Laakso, L., Harrison, R. M., Hanson, I., Leung, C., Lehtinen, K. E. J. and Kerminen, V. M.: Toward direct measurement of atmospheric nucleation, Science (80-.)., 318(5847), 89–92, 2007.

Kulmala, M., Kontkanen, J., Junninen, H., Lehtipalo, K., Manninen, H. E., Nieminen, T., Petäjä, T., Sipilä, M., Schobesberger, S., Rantala, P., Franchin, A., Jokinen, T., Järvinen, E., Äijälä, M., Kangasluoma, J., Hakala, J., Aalto, P. P., Paasonen, P., Mikkilä, J., Vanhanen, J., Aalto, J., Hakola, H., Makkonen, U., Ruuskanen, T., Mauldin, R. L., Duplissy, J., Vehkamäki, H., Bäck, J., Kortelainen, A., Riipinen, I., Kurtén, T., Johnston, M. V., Smith, J. N., Ehn, M., Mentel, T. F., Lehtinen, K. E. J. J., Laaksonen, A., Kerminen, V.-M. M. V.-M., Worsnop, D. R., Petaja, T., Sipila, M., Schobesberger, S., Rantala, P., Franchin, A., Jokinen, T., Jarvinen, E., Aijala, M., Kangasluoma, J., Hakala, J., Aalto, P. P., Paasonen, P., Mikkila, J., Vanhanen, J., Aalto, J., Hakola, H., Makkonen, U., Ruuskanen, T., Mauldin, R. L., Duplissy, J., Vehkamaki, H., Back, J., Kortelainen, A., Riipinen, I., Kurten, T., Johnston, M. V., Smith, J. N., Ehn, M., Mentel, T. F., Lehtinen, K. E. J. J., Laaksonen, A., Kerminen, V.-M. M. V.-M., Worsnop, D. R., Petäjä, T., Sipilä, M., Schobesberger, S., Rantala, P., Franchin, A., Jokinen, T., Järvinen, E., Äijälä, M., Kangasluoma, J., Hakala, J., Aalto, P. P., Paasonen, P., Mikkilä, J., Vanhanen, J., Aalto, J., Hakola, H., Makkonen, U., Ruuskanen, T., Mauldin, R. L., Duplissy, J., Vehkamäki, H., Bäck, J., Kortelainen, A., Riipinen, I., Kurtén, T., Johnston, M. V., Smith, J. N., et al.: Direct observations of atmospheric aerosol nucleation., Science, 339(6122), 943–6, doi:10.1126/science.1227385, 2013.

Kulmala, M., Ezhova, E., Kalliokoski, T., Noe, S., Vesala, T., Lohila, A., Liski, J., Makkonen, R., Bäck, J., Petäjä, T. and Kerminen, V.-M.: CarbonSink+-Accounting for multiple climate feedbacks from forests, Boreal Environ. Res., 25, 145-159, 2020.

Kürten, A., Rondo, L., Ehrhart, S. and Curtius, J.: Calibration of a chemical ionization mass spectrometer for the measurement of gaseous sulfuric acid, J. Phys. Chem. A, 116(24), 6375–6386, doi:10.1021/jp212123n, 2012.

Kürten, A., Jokinen, T., Simon, M., Sipilä, M., Sarnela, N., Junninen, H., Adamov, A., Almeida, J., Amorim,

A., Bianchi, F., Breitenlechner, M., Dommen, J., Donahue, N. M., Duplissy, J., Ehrhart, S., Flagan, R. C., Franchin, A., Hakala, J., Hansel, A., Heinritzi, M., Hutterli, M., Kangasluoma, J., Kirkby, J., Laaksonen, A., Lehtipalo, K., Leiminger, M., Makhmutov, V., Mathot, S., Onnela, A., Petäjä, T., Praplan, A. P., Riccobono, F., Rissanen, M. P., Rondo, L., Schobesberger, S., Seinfeld, J. H., Steiner, G., Tomé, A., Tröstl, J., Winkler, P. M., Williamson, C., Wimmer, D., Ye, P., Baltensperger, U., Carslaw, K. S., Kulmala, M., Worsnop, D. R., Curtius, J. and Barbara Finlayson-Pitts, by J.: Neutral molecular cluster formation of sulfuric acid–dimethylamine observed in real time under atmospheric conditions, Proc. Natl. Acad. Sci. U.S.A., 111(42), 15019–15024, doi:10.1073/pnas.1404853111, 2014.

Kyrö, E. M., Väänänen, R., Kerminen, V. M., Virkkula, A., Petäjä, T., Asmi, A., Dal Maso, M., Nieminen, T., Juhola, S., Shcherbinin, A., Riipinen, I., Lehtipalo, K., Keronen, P., Aalto, P. P., Hari, P. and Kulmala, M.: Trends in new particle formation in eastern Lapland, Finland: Effect of decreasing sulfur emissions from Kola Peninsula, Atmos. Chem. Phys., 14(9), 4383–4396, 2014.

Lai, S. C., Williams, J., Arnold, S. R., Atlas, E. L., Gebhardt, S. and Hoffmann, T.: Iodine containing species in the remote marine boundary layer: A link to oceanic phytoplankton, Geophys. Res. Lett., 38(20), doi:10.1029/2011GL049035, 2011.

Lehtipalo, K., Yan, C., Dada, L., Bianchi, F., Xiao, M., Wagner, R., Stolzenburg, D., Ahonen, L. R., Amorim, A., Baccarini, A., Bauer, P. S., Baumgartner, B., Bergen, A., Bernhammer, A.-K., Breitenlechner, M., Brilke, S., Buchholz, A., Mazon, S. B., Chen, D., Chen, X., Dias, A., Dommen, J., Draper, D. C., Duplissy, J., Ehn, M., Finkenzeller, H., Fischer, L., Frege, C., Fuchs, C., Garmash, O., Gordon, H., Hakala, J., He, X., Heikkinen, L., Heinritzi, M., Helm, J. C., Hofbauer, V., Hoyle, C. R., Jokinen, T., Kangasluoma, J., Kerminen, V.-M., Kim, C., Kirkby, J., Kontkanen, J., Kürten, A., Lawler, M. J., Mai, H., Mathot, S., Mauldin, R. L., Molteni, U., Nichman, L., Nie, W., Nieminen, T., Ojdanic, A., Onnela, A., Passananti, M., Petäjä, T., Piel, F., Pospisilova, V., Quéléver, L. L. J., Rissanen, M. P., Rose, C., Sarnela, N., Schallhart, S., Schuchmann, S., Sengupta, K., Simon, M., Sipilä, M., Tauber, C., Tomé, A., Tröstl, J., Väisänen, O., Vogel, A. L., Volkamer, R., Wagner, A. C., Wang, M., Weitz, L., Wimmer, D., Ye, P., Ylisirniö, A., Zha, Q., Carslaw, K. S., Curtius, J., Donahue, N. M., Flagan, R. C., Hansel, A., Riipinen, I., Virtanen, A., Winkler, P. M., Baltensperger, U., Kulmala, M. and Worsnop, D. R.: Multicomponent new particle formation from sulfuric acid, ammonia, and biogenic vapors, Sci. Adv., 4(12), eaau5363, doi:10.1126/sciadv.aau5363, 2018.

Leino, K., Nieminen, T., Manninen, H. E., Petäjä, T., Kerminen, V.-M. and Kulmala, M.: Intermediate ions as a strong indicator of new particle formation bursts in a boreal forest, Boreal Environ. Res, 21(3-4), 274-286, 2016.

Levasseur, M.: Impact of Arctic meltdown on the microbial cycling of sulphur., Nat. Geosci., 6(9), 691-700, 2013.

Mäkelä, J. M., Aalto, P., Jokinen, V., Pohja, T., Nissinen, A., Palmroth, S., Markkanen, T., Seitsonen, K., Lihavainen, H. and Kulmala, M.: Observations of ultrafine aerosol particle formation and growth in boreal forest, Geophys. Res. Lett., 24(10), 1219–1222, doi:10.1029/97GL00920, 1997.

Manninen, H. E., Mirme, S., Mirme, A., Petäjä, T. and Kulmala, M.: How to reliably detect molecular clusters and nucleation mode particles with Neutral cluster and Air Ion Spectrometer (NAIS), Atmos. Meas. Tech., 9(8), 3577–3605, 2016.

Maso, M. D., Dal Maso, M., Kulmala, M., Riipinen, I., Wagner, R., Hussein, T., Aalto, P. P. and Lehtinen, K. E. J.: Formation and growth of fresh atmospheric aerosols: Eight years of aerosol size distribution data from SMEAR II, Hyytiälä, Finland, Boreal Environ. Res., 10(5), 323–336, 2005.

Mauldin, R., Kosciuch, E., Eisele, F., Huey, G., Tanner, D., Sjostedt, S., Blake, D., Chen, G., Crawford, J. and Davis, D.: South Pole Antarctica observations and modeling results: New insights on HOx radical and sulfur chemistry, Atmos. Environ., 44(4), 572–581, doi:10.1016/j.atmosenv.2009.07.058, 2010.

Mauldin, R. L., Kosciuch, E., Henry, B., Eisele, F. L., Shetter, R., Lefer, B., Chen, G., Davis, D., Huey, G. and Tanner, D.: Measurements of OH, HO2+RO2, H2SO4, and MSA at the South Pole during ISCAT 2000, Atmos. Environ., 38(32), 5423–5437, doi:10.1016/j.atmosenv.2004.06.031, 2004.

McFiggans, G., Bale, C. S. E. E., Ball, S. M., Beames, J. M., Bloss, W. J., Carpenter, L. J., Dorsey, J., Dunk, R., Flynn, M. J., Furneaux, K. L., Gallagher, M. W., Heard, D. E., Hollingsworth, A. M., Hornsby, K., Ingham, T., Jones, C. E., Jones, R. L., Kramer, L. J., Langridge, J. M., Leblanc, C., LeCrane, J. P.-P., Lee, J. D., Leigh, R. J., Longley, I., Mahajan, A. S., Monks, P. S., Oetjen, H., Orr-Ewing, a. J., Plane, J. M. C. C., Potin, P., Shillings, a. J. L. L., Thomas, F., Von Glasow, R., Wada, R., Whalley, L. K. and Whitehead, J. D.: Iodine-mediated coastal particle formation: an overview of the Reactive Halogens in the Marine Boundary Layer (RHaMBLe) Roscoff coastal study, Atmos. Chem. Phys., 10(6), 2975–2999, doi:10.5194/acpd-9-26421-2009, 2010.

Mirme, S. and Mirme, A.: The mathematical principles and design of the NAIS – a spectrometer for the measurement of cluster ion and nanometer aerosol size distributions, Atmos. Meas. Tech., 6(4), 1061–1071, doi:10.5194/amt-6-1061-2013, 2013.

Myllys, N., Ponkkonen, T., Passananti, M., Elm, J., Vehkamäki, H. and Olenius, T.: Guanidine: A Highly Efficient Stabilizer in Atmospheric New-Particle Formation, J. Phys. Chem. A, 122(20), 4717–4729, doi:10.1021/acs.jpca.8b02507, 2018.

Napari, I., Noppel, M., Vehkamäki, H. and Kulmala, M.: Parametrization of ternary nucleation rates for H2so4-NH3-H2O vapors, J. Geophys. Res. Atmos., 107(19), AAC 6-1-AAC 6-6, doi:10.1029/2002JD002132, 2002.

Nieminen, T., Asmi, A., Maso, M. D., Aalto, P. P., Keronen, P., Kulmala, M., Kerminen, V., Dal maso, M., Aalto, P. P., Keronen, P., Petäjä, T., Kulmala, M. and Kerminen, V.: Trends in atmospheric new-particle formation: 16 years of observations in a boreal-forest environment, Boreal Environ. Res., 19 (suppl.(2004), 191–214, 2014.

O'Dowd, C. D., Jimenez, J. L., Bahreini, R., Flagan, R. C., Seinfeld, J. H., Hämerl, K., Pirjola, L., Kulmala, M. and Hoffmann, T.: Marine aerosol formation from biogenic iodine emissions, Nature, 417(6889), 632–636, 2002.

Paasonen, P., Asmi, A., Petäjä, T., Kajos, M. K., Äijälä, M., Junninen, H., Holst, T., Abbatt, J. P. D. D., Arneth, A., Birmili, W., Van Der Gon, H. D., Hamed, A., Hoffer, A., Laakso, L., Laaksonen, A., Richard Leaitch, W., Plass-Dülmer, C., Pryor, S. C., Räisänen, P., Swietlicki, E., Wiedensohler, A., Worsnop, D. R., Kerminen, V.-M. M. and Kulmala, M.: Warming-induced increase in aerosol number concentration likely to moderate climate change, Nat. Geosci., 6(6), 438–442, doi:10.1038/ngeo1800, 2013.

Park, K., Lee, K., Kim, T., Yoon, Y. J., Jang, E., Jang, S., Lee, B. and Hermansen, O.: Atmospheric DMS in the Arctic Ocean and Its Relation to Phytoplankton Biomass, Global Biogeochem. Cycles, 32(3), 351–359, doi:10.1002/2017GB005805, 2018.

Pirjola, L., Laaksonen, A., Aalto, P. and Kulmala, M.: Sulfate aerosol formation in the Arctic boundary layer, J. Geophys. Res. Atmos., 103(D7), 8309–8321, doi:10.1029/97JD03079, 1998.

Raso, A. R. W., Custard, K. D., May, N. W., Tanner, D., Newburn, M. K., Walker, L., Moore, R. J., Huey, L. G., Alexander, L., Shepson, P. B. and Pratt, K. A.: Active molecular iodine photochemistry in the Arctic, Proc. Natl. Acad. Sci. U. S. A., 114(38), 10053–10058, doi:10.1073/pnas.1702803114, 2017.

Reyer, C. P. O., Brouwers, N., Rammig, A., Brook, B. W., Epila, J., Grant, R. F., Holmgren, M., Langerwisch, F., Leuzinger, S., Lucht, W., Medlyn, B., Pfeifer, M., Steinkamp, J., Vanderwel, M. C., Verbeeck, H. and Villela, D. M.: Forest resilience and tipping points at different spatio-temporal scales: Approaches and challenges, J. Ecol., 103(1), 5–15, doi:10.1111/1365-2745.12337, 2015.

Riva, M., Rantala, P., Krechmer, E. J., Peräkylä, O., Zhang, Y., Heikkinen, L., Garmash, O., Yan, C., Kulmala, M., Worsnop, D. and Ehn, M.: Evaluating the performance of five different chemical ionization techniques for detecting gaseous oxygenated organic species, Atmos. Meas. Tech., 12(4), 2403–2421, doi:10.5194/amt-12-2403-2019, 2019.

Ruuskanen, T., Reissell, M., Keronen, A., Aalto, P. P., Laakso, P. P., Grönholm, L., Hari, T. and Kulmala, P.: Atmospheric trace gas and aerosol particle concentration measurements in Eastern Lapland, Boreal Env.

786 Res, 8(4), 335-349, 2003.

787 Ruuskanen, T. M., Kaasik, M., Aalto, P. P., Hõrrak, U., Vana, M., Mårtensson, M., Yoon, Y. J., Keronen, P.,
788 Mordas, G., Ceburnis, D., Nilsson, E. D., O'Dowd, C., Noppel, M., Alliksaar, T., Ivask, J., Sofiev, M.,
789 Prank, M. and Kulmala, M.: Concentrations and fluxes of aerosol particles during the LAPBIAT
790 measurement campaign at Värriö field station, Atmos. Chem. Phys., 7(14), 3683–3700, doi:10.5194/acp-7-
791 3683-2007, 2007.

792 Schmale, J., Zieger, P. and Ekman, A. M. L.: Aerosols in current and future Arctic climate, Nat. Clim.
793 Chang., 11(2), 95–105, doi:10.1038/s41558-020-00969-5, 2021.

794 Seco, R., Holst, T., Sillesen Matzen, M., Westergaard-Nielsen, A., Li, T., Simin, T., Jansen, J., Crill, P.,
795 Friborg, T., Rinne, J. and Rinnan, R.: Volatile organic compound fluxes in a subarctic peatland and lake,
796 Atmos. Chem. Phys., 20(21), 13399–13416, doi:10.5194/ACP-20-13399-2020, 2020.

797 Sherwen, T. M., Evans, M. J., Spracklen, D. V., Carpenter, L. J., Chance, R., Baker, A. R., Schmidt, J. A.
798 and Breider, T. J.: Global modeling of tropospheric iodine aerosol, Geophys. Res. Lett., 43(18), 10012–
799 10019, doi:10.1002/2016gl070062, 2016.

800 Sipilä, M., Sarnela, N., Jokinen, T., Henschel, H., Junninen, H., Kontkanen, J., Richters, S., Kangasluoma, J.,
801 Franchin, A., Peräkylä, O., Rissanen, M. P., Ehn, M., Vehkamäki, H., Kurten, T., Berndt, T., Petäjä, T.,
802 Worsnop, D., Ceburnis, D., Kerminen, V.-M. M., Kulmala, M., O'Dowd, C. and O'Dowd, C.: Molecular-
803 scale evidence of aerosol particle formation via sequential addition of HIO3, Nature, 537(7621), 532–534,
804 doi:10.1038/nature19314, 2016.

805 Sipilä, M., Sarnela, N., Neitola, K., Laitinen, T., Kemppainen, D., Beck, L., Duplissy, E.-M., Kuittinen, S.,
806 Lehmusjärvi, T., Lampilahti, J., Kerminen, V.-M., Lehtipalo, K., Aalto, P., Keronen, P., Siivola, E., Rantala,
807 P., Worsnop, D., Kulmala, M., Jokinen, T. and Petäjä, T.: Wintertime sub-arctic new particle formation from
808 Kola Peninsula sulphur emissions, Atmos. Chem. Phys., 21(23), 17559–17576,
809 doi:https://doi.org/10.5194/acp-21-17559-2021, 2021.

810 Sive, B. C., Varner, R. K., Mao, H., Blake, D. R., Wingenter, O. W. and Talbot, R.: A large terrestrial source
811 of methyl iodide, Geophys. Res. Lett., 34(17), L17808, doi:10.1029/2007gl030528, 2007.

812 Spolaor, A., Barbaro, E., Cappelletti, D., Turetta, C., Mazzola, M., Giardi, F., Björkman, M., Lucchetta, F.,
813 Dallo, F., Pfaffhuber, K. A., Angot, H., Dommergue, A., Maturilli, M., Saiz-Lopez, A., Barbante, C. and
814 Cairns, W.: Diurnal cycle of iodine and mercury concentrations in Svalbard surface snow, Atmos. Chem.
815 Phys. Discuss., 1–25, doi:10.5194/ACP-2019-285, 2019.

816 Stohl, A.: Characteristics of atmospheric transport into the Arctic troposphere, J. Geophys. Res. Atmos., 111,
817 D11306, doi:10.1029/2005JD006888, 2006.

818 Sulo, J., Sarnela, N., Kontkanen, J., Ahonen, L., Paasonen, P., Laurila, T., Jokinen, T., Kangasluoma, J.,
819 Junninen, H., Sipilä, M., Petäjä, T., Kulmala, M. and Lehtipalo, K.: Long-term measurement of sub-
820 3 nm particles and their precursor gases in the boreal forest, Atmos. Chem. Phys., 21(2), 695–715,
821 doi:10.5194/acp-21-695-2021, 2021.

822 Tarvainen, V., Hakola, H., Hellén, H., Bäck, J., Hari, P. and Kulmala, M.: Temperature and light dependence
823 of the VOC emissions of Scots pine, Atmos. Chem. Phys., 4(5), 989-998, doi: 10.5194/acp-5-989-2005,
824 2004.

825 Tiiva, P., Faubert, P., Michelsen, A., Holopainen, T., Holopainen, J. K. and Rinnan, R.: Climatic warming
826 increases isoprene emission from a subarctic heath, New Phytol., 180(4), 853–863, doi:10.1111/J.1469-
827 8137.2008.02587.X, 2008.

828 Tunved, P., Hansson, H. C., Kerminen, V. M., Ström, J., Dal Maso, M., Lihavainen, H., Viisanen, Y., Aalto,
829 P. P., Komppula, M. and Kulmala, M.: High natural aerosol loading over boreal forests, Science (80-.).,
830 312(5771), 261–263, doi:10.1126/science.1123052, 2006.

831 Valolahti, H., Kivimäenpää, M., Faubert, P., Michelsen, A. and Rinnan, R.: Climate change-induced

vegetation change as a driver of increased subarctic biogenic volatile organic compound emissions, Glob. Chang. Biol., 21(9), 3478–3488, doi:10.1111/GCB.12953, 2015.

Vana, M., Komsaare, K., Hõrrak, U., Mirme, S., Nieminen, T., Kontkanen, J., Manninen, H. E., Petäjä, T., Noe, S. M. and Kulmala, M.: Characteristics of new-particle formation at three SMEAR stations, Boreal Environ. Res., 21(3-4), 345-362, 2016.

Vehkamäki, H., Dal Maso, M., Hussein, T., Flanagan, R., Hyvärinen, A., Lauros, J., Merikanto, J., Mönkkönen, P., Pihlatie, M., Salminen, K., Sogacheva, L., Thum, T., Ruuskanen, T. M., Keronen, P., Aalto, P. P., Hari, P., Lehtinen, K. E. J., Rannik, Ü. and Kulmala, M.: Atmospheric particle formation events at Värriö measurement station in Finnish Lapland 1998-2002, Atmos. Chem. Phys., 4(7), 2015–2023, doi:10.5194/acp-4-2015-2004, 2004.

Wang, S., Riva, M., Yan, C., Ehn, M. and Wang, L.: Primary Formation of Highly Oxidized Multifunctional Products in the OH-Initiated Oxidation of Isoprene: A Combined Theoretical and Experimental Study, Environ. Sci. Technol., 52(21), 12255–12264, doi:10.1021/acs.est.8b02783, 2018.

Wang, Y. Q., Zhang, X. Y. and Draxler, R. R.: TrajStat: GIS-based software that uses various trajectory statistical analysis methods to identify potential sources from long-term air pollution measurement data, Environ. Model. Softw., 24(8), 938–939, doi:10.1016/j.envsoft.2009.01.004, 2009.

Yan, C., Nie, W., Aïjälä, M., Rissanen, M. P., Canagaratna, M. R., Massoli, P., Junninen, H., Jokinen, T., Sarnela, N., Häme, S. A. K. K., Schobesberger, S., Canonaco, F., Yao, L., Prévôt, A. S. H. H., Petäjä, T., Kulmala, M., Sipilä, M., Worsnop, D. R., Ehn, M., Äijälä, M., Rissanen, M. P., Canagaratna, M. R., Massoli, P., Junninen, H., Jokinen, T., Sarnela, N., Häme, S. A. K. K., Schobesberger, S., Canonaco, F., Yao, L., Prévôt, A. S. H. H., Petäjä, T., Kulmala, M., Sipilä, M., Worsnop, D. R. and Ehn, M.: Source characterization of highly oxidized multifunctional compounds in a boreal forest environment using positive matrix factorization, Atmos. Chem. Phys., 16(19), 12715–12731, doi:10.5194/acp-16-12715-2016, 2016.

Yu, H., Ren, L., Huang, X., Xie, M., He, J. and Xiao, H.: Iodine speciation and size distribution in ambient aerosols at a coastal new particle formation hotspot in China, Atmos. Chem. Phys., 19(6), 4025–4039, doi:10.5194/acp-19-4025-2019, 2019.